Carbohydrate Polymer Technologies and Applications 7 (2024) 100508

Contents lists available at ScienceDirect

Carbohydrate Polymer Technologies and Applications

journal homepage: www.sciencedirect.com/journal/carbohydrate-polymer-technologies-and-applications

Industrial byproduct pine nut skin factorial design optimization for production of subcritical water extracts rich in pectic polysaccharides, xyloglucans, and phenolic compounds by microwave extraction

Soraia P. Silva [a], Pedro Ferreira-Santos [b,c], Guido R. Lopes [a], Sofia F. Reis [a], Abigail González [d], Clarisse Nobre [d,e], Victor Freitas [f], Manuel A. Coimbra [a], Elisabete Coelho [a,*]

[a] LAQV-REQUIMTE, Department of Chemistry, University of Aveiro, 3810-193, Aveiro, Portugal
[b] Department of Chemical Engineering, Faculty of Science, University of Vigo, As Lagoas, Ourense, 32004, Spain
[c] IAA - Instituto de Agroecoloxía e Alimentación, University of Vigo (Campus Auga), As Lagoas, 32004, Ourense, Spain
[d] CEB - Centre of Biological Engineering, University of Minho, Braga, 4710-057, Portugal
[e] LABBELS – Associate Laboratory, Braga, Guimarães, Portugal
[f] LAQV-REQUIMTE, Departamento de Química e Bioquímica, Faculdade de Ciências da Universidade do Porto, Rua do Campo Alegre, 689, Porto, Portugal

ARTICLE INFO

Keywords:
Soluble dietary fiber
Auto-hydrolysis
Hydrothermal treatment
Gastrointestinal stability
Cutin
Microwave-assisted extraction
Full factorial design optimization

ABSTRACT

Pine nut skin (*Pinus pinea* L.) is a poorly explored industrial byproduct with potential to be utilized as a food ingredient. Subcritical water extraction (SWE), an eco-friendly extraction technique with higher efficiency than hot-water extraction (HWE), was studied to evaluate its suitability in producing extracts rich in soluble fiber and phenolic compounds. For this, a factorial design was developed considering temperature (120–180 °C), time (2–10 min), and mass/volume ratio (1–3 g/60 mL) under microwave irradiation. This design aimed to maximize the extraction of carbohydrates, while achieving the highest content of phenolic compounds and antioxidant activity. SWE produced higher yields (2.6-fold in relation to HWE) of extracts rich in polysaccharides, determined by methylation analysis, oligosaccharides, determined by GC-qMS as alditol acetates, and phenolic compounds, determined by HPLC-ESI-MS. SWE increased the recovery of pectic oligosaccharides (10-fold) and xyloglucans (2-fold), and allowed to recover pectic polysaccharides, type II arabinogalactans and insoluble-bound phenolic compounds. Mono-, oligo- and polysaccharides were not hydrolyzed during *in vitro* gastrointestinal digestion, showing potential prebiotic functionality. Although phenolic compounds suffered a 23 % (gallic acid equivalents) decrease, phenolic acids and aldehydes were released or conserved upon intestinal phase. These results highlight the potential of PNS valorization as functional food ingredients through the subcritical water solubilization of polysaccharides and phenolic compounds.

1. Introduction

The industrial processing of pine nut generates high volumes of byproducts, namely the cone, nutshells, and the outer skin, as it only concerns 3–5 % of the pinecone (Loewe-Muñoz et al., 2019). From the arising byproducts, pine nut skin (PNS) is a food grade component, although usually removed before pine nut commercialization. PNS, together with the remaining byproducts, are usually used for energy production (Adelina et al., 2022; Queirós et al., 2020), which is amongst the least preferable use of the food waste management hierarchy (Moshtaghian et al., 2021). The limited studies on PNS, only dedicated to the characterization of phenolic compounds and antioxidant activity (Adelina et al., 2022; Zhao et al., 2017), do not allow the current exploitation of this byproduct beyond these compounds, namely the use of dietary fiber as a food ingredient.

Nut skins, in general, are a rich source of dietary fiber, mostly in its insoluble form, and of phenolic compounds (Mandalari et al., 2010; Özdemir et al., 2014; Silva et al., 2024). Dietary fiber is defined as the plant components that are resistant to digestion and can undergo fermentation in the large intestine, namely cellulose, xyloglucans and other hemicelluloses, pectic polysaccharides, and lignin (Stribling & Ibrahim, 2023). Xyloglucans are the most abundant hemicellulose structure found in gymnosperms primary cell wall (about 20 %) (Pękala et al., 2023), composed of (β1,4)-D-glucopyranosyl residues substituted

* Corresponding author.
E-mail address: ecoelho@ua.pt (E. Coelho).

https://doi.org/10.1016/j.carpta.2024.100508

Available online 7 May 2024

at *O*-6 with α-D-Xyl*p*, that may be further substituted at *O*-2 by β-D-Gal*p* units, which in turn can be linked at *O*-2 to α-L-Fuc*p* residues (Tuomivaara et al., 2015). Pectic polysaccharides are characterized by the presence of galacturonic acid (GalA), with a linear homopolymer composed of (α1,4)-D-Gal*p*A, which can be methyl-esterified and acetylated. Rhamnose is also a component of pectic polysaccharides, forming the backbone of the repeating disaccharide [→4)-α-D-Gal*p*A-(1→2)-α-L-Rha*p*-(1→]$_n$, which can be substituted at *O*-4 position of Rha*p* by arabinans, galactans, and arabinogalactans (Mohnen, 2008). The consumption of these polysaccharides has been associated to several health-related outcomes, such as improved colonic health, blood cholesterol levels, and glucose metabolism (Bai & Gilbert, 2022; Cantu-Jungles et al., 2019; Cheng et al., 2020; Lee et al., 2022).

Phenolic compounds can occur covalently linked (ester, ether and C–C bonds) to dietary fiber structures, namely carbohydrates and lignin, and to cutin, as insoluble-bound compounds, and as free and soluble-bound (glycosides) forms, which are easily extracted by solvents (Acosta-Estrada et al., 2014; Kong et al., 2020). Considering the composition of nut skins, PNS could be utilized as a source of functional food ingredients, bringing benefits for the pine nut industry, for the consumers seeking well-being maintenance through bioactive compounds consumption, and for the environment by promotion of resources efficiency.

The utilization of water-based extraction methodologies contributes to the pursuit of a more sustainable process and allows to utilize the extracts as food ingredients. However, nut skins are mostly insoluble, which difficult the recovery of bioactive compounds. Subcritical water extraction (SWE) is environmentally friendly, as water substitutes the toxic and hazardous organic solvents (Smith, 2002). Under subcritical water conditions, water is heated above its boiling point (100 °C, 1 atm) without reaching its supercritical state (374 °C) and kept under sufficient pressure to maintain its liquid state. Under these conditions, the water ionization constant (Kw) increases, and water becomes more acidic, resulting in a more hydrolytic solvent. Thus, subcritical water possesses solvent properties highly suitable for the extraction of carbohydrates and phenolic compounds from insoluble matrices (Erşan et al., 2018; Ravber et al., 2015).

This study hypothesizes that through subcritical water treatment it is possible to use pine nut skin, an insoluble and low-value industrial byproduct, as a source of food ingredients rich in soluble polysaccharides, oligosaccharides, and phenolic compounds. The SWE conditions were optimized to maximize carbohydrates, together with high phenolic compounds content and antioxidant activity, and the results compared with those obtained by hot water extraction (HWE). The carbohydrates and phenolic compounds were characterized by GC-qMS and HPLC−DAD/ESI-MS coupled to an LTQ Orbitrap. Their stability was studied in an *in vitro* digestion model, allowing to evaluate their potential use as functional food ingredients.

2. Material and methods

2.1. Standards and reagents

Folin–Ciocalteu reagent, gallic acid, acetic anhydride, NaOH, KCl, $CaCl_2 \cdot (H_2O)_2$, KH_2PO_4 and NaCl were purchased in PanReac (Barcelona, Spain). ABTS (2,2′-azino-bis-(3- thylbenzothiazolne-6-sulfonic acid) diammonium salt), ascorbic acid, $NaBD_4$, 1-methylimidazole, trifluoroacetic acid (TFA), CH_3I, vanillin, arabinose, 2-deoxyglucose, xylose, glucose, sucrose, porcine pepsin, pancreatin, bile extract porcine, HCl, $NaHCO_3$, $(NH_4)_2CO_3$ were obtained from Sigma Aldrich (St. Louis, MO, USA). Methanol (HPLC grade), $NaBH_4$, and *m*-phenylphenol were acquired from Fisher Scientific (Waltham, MA, USA). Ethanol, acetone and formic acid (puriss. p.a. for mass spectroscopy) were provided by Honeywell (Charlotte, NC, USA). Arabinobiose, cellobiose, xylotriose and mannotriose were obtained from Megazyme (Bray, Ireland). Acetic acid and H_2SO_4 were purchased from Carlo Erba (Milan, Italy) and ChemLab (Zedelgem, Belgium), respectively. D-Galacturonic acid and $MgCl_2 \cdot (H_2O)_6$ were otbtained from Merck (Darmstadt, Germany). Filters (nylon, 0.45 μm) were obtained from Labbox (Barcelona, Spain) and dialysis membranes, with a 12–14 kDa cut-off, from Medicell Membranes Ltd. (London, England).

2.2. Sample preparation

Pine nut (*Pinus pinea* L.) skins were kindly provided by PineFlavour Lda. (Grândola, Portugal). This byproduct was recovered during the pine nut processing after washing and drying through a suction system. Pine nut skins (PNS) were milled and sieved (500 μm), arising two particle sizes, PNS-C (coarse, ≥ 500 μm) and PNS-F (fine, < 500 μm) (Silva et al., 2024). Samples were stored at 4 °C until analyses.

2.3. Subcritical-water extraction (SWE) using a microwave heating system

PNS-F (< 500 μm) was used for the optimization of the subcritical-water extraction (SWE) conditions, due to its higher availability (yield of 85 % of PNS sample), homogeneity, and higher extractability given to an increased surface area. The SWE experiments were carried out using a microwave oven - MicroSYNTH Labstation (maximum output, 1 kW, 2.45 GHz; Milestone Inc., Shelton, CT). The temperature is adjusted by a PID (Proportional, Integral, Derivative) algorithm by changing the power of microwave irradiation (Passos & Coimbra, 2013). Powdered samples were placed in the reactors and dispersed in 60 mL of distilled water. The desired temperature was attained in 2 min and maintained throughout the experiment (Lopes et al., 2020). The reactors were cooled down and the extracts, vacuum filtered (1.2 μm glass microfiber filter), frozen, and freeze-dried.

2.3.1. Design of experiments

A full factorial design was used to optimize the SWE conditions, namely temperature (°C), time (min), and m/v ratio (g/60 mL) at 2 levels, low and high coded (−1) and (+1), respectively. Additionally, 3 replicates of the center point, coded (0), were used to estimate the curvature of the response surface and the pure error of the experiment. The 2^3 full factorial design with 3 center points totalized an 11-run experiment, with equipment duplicates (two reactors in each experiment) and in a random order (**Table S1**). After preliminary testing revealed that high m/v ratios (3 g/60 mL) combined with high temperatures (200 °C) result in overpressure (over 55 bar), the extreme conditions were established.

The data obtained were adjusted to a first-order model represented by the Eq. (1):

$$Y_n = \beta_{n0} + \sum_{i=1}^{3} \beta_{ni} X_i + \sum_{i=1}^{2} \sum_{j=i+1}^{3} \beta_{nij} X_i X_j \quad (1)$$

where Y_n is the response variable, X_i and X_j are the factors (temperature, time, m/V ratio), β_{n0} is the intercept, and β_{ni}, β_{nj}, and β_{nij} are the coefficients that represent the main and interaction effects of the factors. The dependent variables were extraction yield (%, w/w), carbohydrates (mg/g extract), total phenolic compounds (TPC) (mg gallic acid equivalents/g extract), and antioxidant activity (ABTS) (mg ascorbic acid equivalents/g extract). The equation's coefficients were determined using factorial regression analysis (Minitab v17 software program), by analysis of variance with a 95 % confidence interval, and the model was used to establish the ideal factor levels to maximize the response variables. Models' validation was performed by 4 replicates.

2.3.2. SWE laboratorial scale-up

To scale up the extraction process, the number of reactors on the microwave apparatus was increased from 2 to 8, and the heating step was extended to 12 min to allow the uniform heating of all reactors. The

established optimum conditions were utilized during the scale-up extraction of unfractionated PNS samples, and the resulting responses were compared to those obtained during the optimization process to determine the impact of the process upscale.

2.4. Hot water extraction (HWE)

Powdered PNS-F fraction (< 500 μm) was water-extracted using a m/v ratio of 1 g/60 mL in a covered Erlenmeyer flask, at 100 °C with magnetic agitation, during 30 min. After extraction, the mixture was cooled down to room temperature (20 °C) and vacuum filtered (1.2 μm glass microfiber filter), frozen and freeze-dried. The HWE extracts were evaluated for the same responses as SWE extracts to compare the two extraction methodologies. HWE was scaled up by using unfractionated PNS samples and increasing the m/v ratio to 3 g/60 mL.

2.5. Sequential extraction of phenolic compounds from pine nut skin fractions

Extraction was performed sequentially on 5 g of defatted PNS-F and PNS-C with 80 % ethanol, in a proportion of 1:20 (w/V, g/mL), 10 min, 60 °C. The obtained residue was extracted 5 times with acetone/water/acetic acid (60/39/1, V/V/V) in a proportion of 1/10 (w/V, g/mL), 60 min, 20 °C. Filtered and freeze-dried extracts were dissolved in 10 mL of acidic water (pH 2) and extracted 4 times with 10 mL of ethyl acetate (Mandalari et al., 2010). Free and soluble-bound phenolic compounds were recovered in the organic phases, after vigorous shake and centrifugation (15,892 × *g*, 4 °C, 15 min), were combined, dried, and placed in a vacuum desiccator at 20 °C, until constant weight. The aqueous phases were purified by solid phase extraction (SPE) using Sephadex LH-20. Before loading the sample, the column (bed weight 2 g, volume 12 mL) was preconditioned with 24 mL of methanol followed by 24 mL of water. After sample loading, the column was washed with 24 mL of water and the tannin-rich fraction was eluted with 24 mL of a mixture of methanol/acetone/water (3:1:1, V/V/V), and evaporated to dryness (Reis et al., 2019). Proanthocyanidins monomers were determined after hydrolysis of the tannin-rich fractions. Samples (1 mg) were added to 1 mL of 2 M HCl (prepared in methanol) for 2 h at 100 °C (Reis et al., 2019). The reaction was stopped in an ice bath, filtered (nylon, 0.45 μm) and injected in an UltiMate™ 3000 UHPLC Dionex Thermo Scientific system (Waltham, Massachusetts, EUA), using an RP-18 5 μm, LiChrospher® 100 (LiChro-CART® 250–4) column at 25 °C. The mobile phase was water/formic acid (99:0.1; V/V) (eluent A) and methanol/formic acid (99:0.1; V/V) (eluent B), with a flow rate of 1 mL/min. The elution started at 95 % solvent A to 0 % in 20 min, was kept for 5 min, reached 95 % solvent A in 1 min, and was kept for 9 min. The absorbance detection was set to 520 nm and data processing was achieved by Chromeleon™ Chromatography Data System (CDS) software (Reis et al., 2019).

The residues obtained after sequential extraction (ethanol and acetone) were analyzed for cell-wall ester-linked phenolic compounds, by extraction with 4 M NaOH (1:200 g/mL) overnight (16 h), at 20 °C (Mandalari et al., 2010). The pH was adjusted to 2 prior extractions with ethyl acetate. The aqueous phase was centrifuged and purified by SPE, as aforementioned.

Phenolic compounds extraction scheme is exhibited in **Figure S1**, showing the obtained yields for each step.

2.6. Ethanol precipitation

The SWE and HWE extracts, obtained after scale-up (Sections 2.3.2 and 2.4), were prepared at a concentration of 10 mg/mL in water. The resulting mixture was then subjected to centrifugation at 24,652 × *g*, for 10 min, at 4 °C to remove any insoluble material. Ethanol (EtOH) was gradually added to the supernatant (Sn) to reach concentrations between 50 % and 90 %. Mixtures were allowed to settle at 4 °C, overnight (16 h), followed by centrifugation to remove the precipitate. Precipitation occurred only at 75 % EtOH, and the EtOH was removed from the supernatants and precipitates through rota-evaporation at 40 °C, and then freeze-dried (Coimbra et al., 1996). The resulting supernatants were designated as EtSn and the precipitates as Et75.

2.7. Carbohydrates analysis

2.7.1. Neutral sugars and uronic acids

Neutral sugars were analyzed by gas chromatography-flame ionization detection (GC-FID), after conversion to their alditol acetates, as previously described (Añibarro-Ortega et al., 2019; Lopes et al., 2016). Samples (1–2 mg) were pre-hydrolyzed in 0.2 mL of 72 % (w/w) H_2SO_4 for 3 h at 20 °C, followed by hydrolysis in 1 M H_2SO_4 at 100 °C for 2.5 h for the release of monosaccharides from polysaccharides. Monosaccharides were reduced ($NaBH_4$) and acetylated (acetic anhydride using methyl imidazole as the catalyst). The alditol acetates were analyzed using a DB-225 column (30 m, 0.25 mm i.d., 0.25 μm film thickness) and a GC-FID PerkinElmer-Clarus 400. The temperature of the injector was 220 °C while the detector operated at 230 °C. The following oven temperature program was used: initial temperature of 200 °C, rise to 220 °C at 40 °C/min, standing for 7 min, and rise to 230 °C. The carrier gas (H_2) had a flow rate set at 1.7 mL/min.

Uronic acids were determined using the *m*-phenylphenol colorimetric method (Cruz et al., 2018). After pre-hydrolysis (0.2 mL of 72 % H_2SO_4 for 3 h at 20 °C), samples were hydrolyzed for 1 h in 1 M H_2SO_4 at 100 °C. The hydrolyzed samples were diluted (1:4, V/V) and 3 mL of 200 mM boric acid prepared in H_2SO_4 98 % (w/w) was added to 0.5 mL of each sample. The mixture was shaken and heated at 100 °C for 10 min. After cooling on ice, 100 μL of *m*-phenylphenol was added, and the absorbance was measured at 520 nm. For quantification, the calibration curve was made with D-galacturonic acid (0–100 μg/mL, 6 calibration points), and the results were expressed as GalA equivalents.

2.7.2. Free sugars

Free sugars were analyzed as described for neutral sugars, without the hydrolysis step. The alditol acetates, with a degree of polymerization (DP) up to 5, were identified and quantified by adapting the gas chromatography-quadrupole mass spectrometry (GC-qMS) to high operating temperatures (Imperio et al., 2021; Roupar et al., 2022). For the volatilization of high molecular weight derivatives, the injection port was set to 400 °C and its components (inlet, septum, O-ring) were high-temperature resistant. The high-temperature capillary column HT5 (30 m of length, 0.25 mm of internal diameter, 0.10 μm of film thickness) (Trajan Scientific, Victoria, Australia), was used with the previously reported oven temperature program (Roupar et al., 2022). For quantitative analysis, relative response factors of arabinose, xylose, glucose, arabinobiose, sucrose, cellobiose, xylotriose, and mannotriose to 2-deoxyglucose were determined.

2.7.3. Glycosidic-linkage analysis

Samples were dissolved in anhydrous dimethylsulfoxide, and powdered NaOH was added under an argon atmosphere. Carbohydrates were methylated with CH_3I (3-times 70 μL, 20-min, stirring), dissolved in 3 mL chloroform:methanol (1:1, V/V) and dialyzed (12–14 kDa) against 50 % EtOH, at 20 °C. The material retained within the dialysis membranes was dried, and the prior procedure was repeated to assure the methylation of all the free hydroxyl groups. The glycosidic linkages were then hydrolyzed with 1 mL of 2 M TFA at 120 °C for 1 h, and the acid was completely evaporated. The resultant monosaccharides were reduced with $NaBD_4$ and acetylated. The partially methylated alditol acetates were identified by GC-qMS (GC-2010 Plus, Shimadzu, Japan) with the chromatographic conditions already reported (Gudiña et al., 2022).

2.8. Phenol-sulfuric acid method

Total sugar content of the design of experiments resulting extracts was determined according to a modification of the phenol-sulfuric acid method (DuBois et al., 1956), by addition of 80 μL of sample (300 mg/L) dissolved in water, followed by 160 μL of phenol 5 % (w/v) and 1 mL of H_2SO_4 96 %, using glucose as standard (0–240 mg/L, 9 calibration points).

2.9. Phenolic compounds characterization

The identification/tentative identification of phenolic compounds obtained after extraction and ethyl acetate purification was performed using a HPLC−DAD/Electrospray Ionization-Mass Spectrometry (ESI-MS) coupled to an LTQ Orbitrap XL (Thermo Fischer Scientific, Bremen, Germany), as previously described (Reis et al., 2019). Compounds were separated on a reversed phase silica column RP-18 5 μm, Purospher®-STAR (LiChroCART® 150–4.6) and the solvents used were water/formic acid (99:1, V/V) (solvent A) and acetonitrile/formic acid (99:1, V/V) (solvent B). Column temperature was maintained at 25 °C. A stepwise gradient from 1 to 31 % solvent B was applied at a flow rate of 0.45 mL/min for 6 min, reached 100 % B at 30 min, kept for 4 min, and decreased to 1 % B in 3 min and kept for 3 min.

Phenolic compounds quantification was carried out using a 1260 Infinity LC (Agilent Technologies, Palo Alto, CA, USA), coupled to an AB SCIEX Triple Quad 3500 (AB Sciex, Foster City, CA) electrospray ionization source (ESI). Samples were freeze-dried and reconstituted in methanol, before injection (5 μL). Compounds were separated using a C18 3 μm, Phenomenex Luna® (150 mm × 2 mm) column, as already reported (Del-Castillo-Llamosas et al., 2023) .

2.10. Folin–Ciocalteu method for total polyphenol quantification

Deionized water, Folin–Ciocalteu reagent (Sigma), and sample dissolved in water were sequentially added to a microplate (60, 15, and 15 μL, respectively), reacted for 5 min, followed by addition of 150 μL 7 % Na_2CO_3. The absorbance was measured at 750 nm, after 60 min, at 30 °C, in the dark (Singleton & Rossi, 1965). The results were expressed as mg/g of gallic acid equivalents (GAE), using a concentration range of 0–250 mg/L (12 calibration points).

2.11. Proanthocyanidins quantification

The total proanthocyanidin content was determined according to the vanillin assay (Sun et al., 1998). In a microplate, 40 μL of samples (1 mg/mL MeOH) was mixed with 100 μL of vanillin (1 g/100 mL MeOH) and 100 μL of H_2SO_4 (10 mL/100 mL MeOH), and reacted for 15 min at 30 °C. All solutions were prepared in methanol as water interfere with the reaction. Blanks were performed for each sample, with the substitution of vanillin by methanol. The results were expressed as mg/g of catechin equivalents (CE), using a concentration range between 0 and 300 mg/L (10 calibration points).

2.12. Antioxidant activity by ABTS method

The antioxidant activity was measured using the 2,2′-azinobis-3-ethylbenzothiazoline-6-sulfonic acid (ABTS) assay (Re et al., 1999). To generate the radical cation ($ABTS^{\bullet+}$), an aqueous solution of potassium persulfate (660 mg/L) was mixed with ABTS stock solution (3.8 g/L) and left in the dark at 20 °C for 12–16 h. The $ABTS^{\bullet+}$ solution was diluted with water to an absorbance of 0.700 at 734 nm, and 250 μL of this solution were mixed with 50 μL of sample or standard and left to react for 15 min in the dark. The results were expressed as mg/g of ascorbic acid equivalents (AAE), using a concentration range between 0 and 57 mg/L (8 calibration points).

2.13. In vitro digestion

EtSn and Et75 fractions from HWE and SWE were digested using the harmonized INFOGEST 2.0 protocol (static *in vitro* gastrointestinal digestion) simulating the mouth, stomach, and small intestine conditions (**Table S2**) (Brodkorb et al., 2019; Ferreira-Santos et al., 2024).

Samples (1 g) were dispersed in 5 mL of ultrapure water at 37 °C and added to simulated salivary fluid (SSF) solution and $CaCl_2{\cdot}(H_2O)_2$ (final concentration of 1.5 mM in the fluid) to simulate mouth conditions. As the samples did not contain starch, α-amylase was not added. After incubation at 37 °C for 2 min, 1 mL was sampled and cooled down on ice for analysis.

For the stomach phase, simulated gastric fluid (SGF) solution, porcine pepsin solution (final activity of 2000 U/mL), and $CaCl_2{\cdot}(H_2O)_2$ (0.15 mM) were added. The pH was adjusted to 3 using HCl (1 M) and incubated for 2 h at 37 °C. Aliquots of 1 mL were taken and cooled on ice to stop the enzymatic reaction.

In the intestinal phase, simulated intestinal fluid (SIF) solution, $CaCl_2{\cdot}(H_2O)_2$ (0.6 mM), pancreatin (100 U/mL), and bile solutions (10 mM in the final volume) were added. The pH was adjusted to 7 using NaOH (1 M), and the mixture was incubated for 2 h at 37 °C. The digestion was stopped by cooling on ice. All aliquots were stored at −20 °C until analyses. Samples were digested in triplicate. A blank (water without the sample) was incubated under the same conditions and used to correct interferences from digestive enzymes and buffers for further analysis.

3. Results and discussion

3.1. Subcritical water extraction of pine nut skin

Subcritical water extraction (SWE) was used to extract carbohydrates and phenolic compounds from pine nut skin (fine fraction, < 500 μm). To maximize the extraction, high temperature, longtime of irradiation, and high mass of pine nut skin to volume of water was tested. It was possible to observe that a temperature of 200 °C during 4 min, using a m/V ratio of 3 g/60 mL, resulted in overpressure (over 55 bar). Based on these extreme conditions observed, it was constructed a 2^3 full factorial design with 3 center points with temperatures of 120 °C, 150 °C and 180 °C, time of 1, 5.5 and 10 min, and m/v ratios of 1, 2 and 3 g/60 mL (**Table S1**). The experimental values obtained for extraction yield, total carbohydrates, total phenolic compounds, and antioxidant activity are represented in Fig. 1 and **Table S1**. The data obtained were adjusted to a first-order model, and the equation's coefficients were determined using factorial regression analyses. For comparison purposes, a hot water extraction (HWE) was performed at 100 °C, for 30 min, and a m/V of 1 g/60 mL. These conditions were used as longer extraction times (4 h with solvent renovation after 2 h) with a higher m/v ratio (3 g/60 mL) resulted in minimal increase (7 %) in the extraction yield.

The extraction yield ranged from 6.8 % (120 °C, 1 min, 3 g/60 mL) to 19.0 % (180 °C, 1 min, 1 g/60 mL). Temperature was the sole factor with a positive impact on the extraction yield ($p < 0.0001$), while m/V ratio had a negative impact ($p = 0.001$) (Fig. 1a). HWE yield was 7.7 ± 0.13 % (Fig. 1a, dotted line), which was comparable ($p = 0.61$) to the values obtained by SWE when temperature was 120 °C (8.0 ± 0.93 %).

Total carbohydrates of the extracts ranged from 137 to 362 mg/g (Fig. 1b), showing a 2.6-fold variation from the extraction at 120 °C, 10 min, 3 g/60 mL to the extraction at 180 °C, 10 min, 3 g/60 mL (**Table S1**). This confirms temperature as a preponderant factor, positively influencing the carbohydrate's extraction ($p < 0.0001$) (Fig. 1b). Time and interaction between temperature and time had a positive effect on this response as well, which indicates that the temperature effect was more evident when the extraction time was longer. HWE produced an extract with a carbohydrate content of 179 ± 4.10 mg/g, which is equivalent ($p = 0.19$) to the values obtained by SWE when the temperature was 120 °C (161 ± 10 mg/g), independently of time and m/V

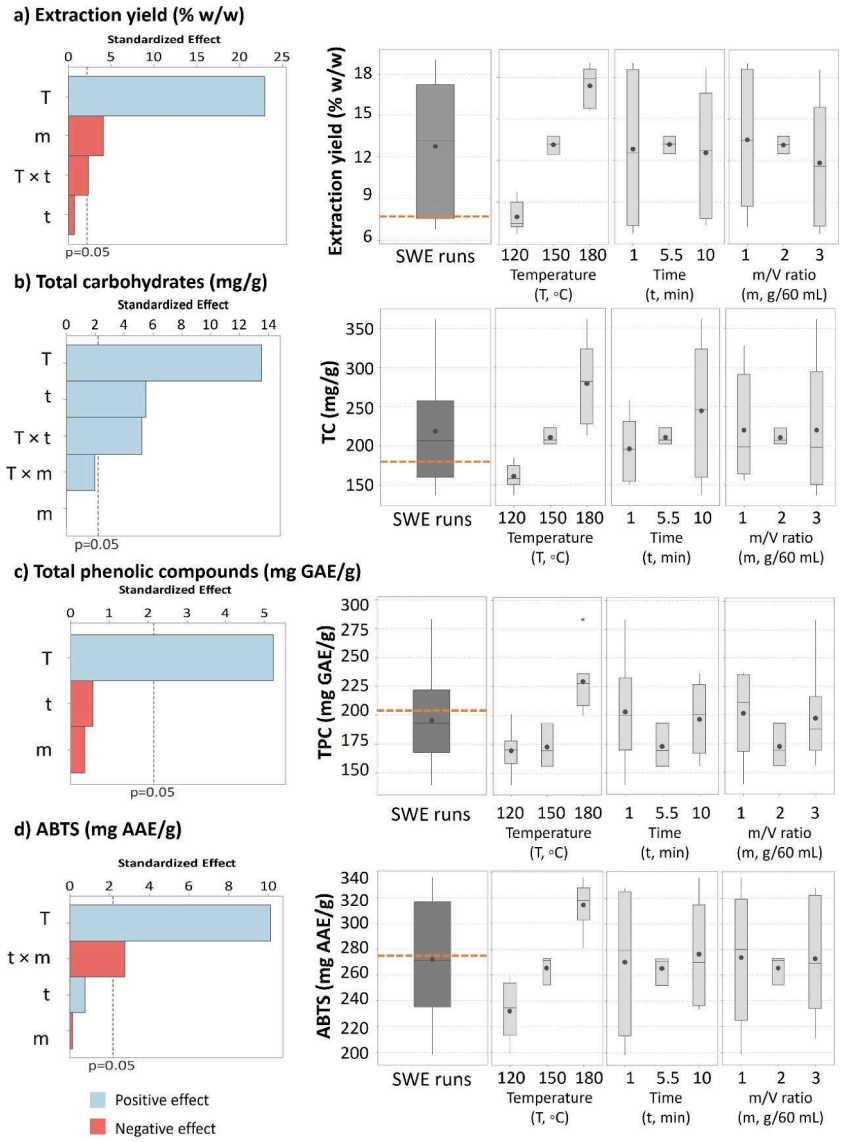

Fig. 1. Pareto charts (left) and box plots (right), after models' reduction, of temperature (T), time (t), and m/v ratio (m) during the SWE on the (a) extraction yield (w/w %), (b) total carbohydrates (mg/g), (c) TPC (GAE mg/g), and (d) ABTS (AAE mg/g) of the obtained extracts. In the Pareto chart, the negative and positive effects are highlighted in blue and red, respectively, and the statistical significance (p-value) is defined by the vertical line. Box plots show the distribution of the raw data, containing the box the interquartile range and limiting the whisker the non-outlier range, with the median represented as (-), the mean as (●), and outliers as (*), while HWE (100 °C, 30 min, 1 g/60 mL) results are represented by the dotted line.

ratio used in SWE.

The phenolic compounds extraction was solely affected by temperature (120–180 °C). The same range of phenolic compounds was observed at 120 °C and 150 °C (140–201 mg GAE/g), and the increase was only observed at 180 °C (200–236 mg GAE/g (Fig. 1c). HWE yielded a TPC content of 202 mg GAE/g, which is higher than the yield obtained with the experiments using 120 °C ($p < 0.05$), but below the results achieved at 180 °C. It is possible that only free and soluble-bound phenolic compounds were extracted by HWE and SWE at 120 °C. In that case, the lower extraction times used in SWE (2–10 min) resulted in the extraction of lower amounts of phenolic compounds.

The antioxidant activity (ABTS) ranged from 198 mg AAE/g (120 °C, 1 min, 1 g/60 mL) to 335 mg AAE (180 °C, 10 min, 1 g/60 mL) (Fig. 1d). The positive effect of temperature on this response was observed by the 1.4-fold increase between the mean of the conditions using 120 °C and 180 °C. The interaction between time and m/V ratio had a negative effect on the extract's antioxidant activity, increasing with time when the w/V ratio is low (1 g/60 mL) and decreasing with time when the w/V ratio is high (3 g/60 mL). This effect was not observed for TPC, which may be explained by the distinct reaction mechanisms of Folin–Ciocalteu (TPC) and the ABTS assays. HWE produced extracts with higher antioxidant activity than SWE at 120 °C, as observed for TPC. In this case it was observed a positive correlation between TPC and ABTS ($r = 0.84$, $p < 0.0001$).

These results showed that the cleavage of carbohydrates and phenolic compounds from pine nut skin was highly increased when drastic temperatures were applied. This is in accordance with works where the extraction of polysaccharides from lignocellulosic matrices is optimal at 180 °C, under subcritical water conditions, while promote the cleavage of the bound phenolic compounds to hemicelluloses, resulting in their extraction (Cocero et al., 2018).

The full factorial models demonstrated statistical significance ($p < 0.001$), with non-significant lack-of-fit ($p > 0.05$) and no significant evidence of curvature (non-linearity) ($p > 0.05$) for all responses (**Table S3**). This suggests that the obtained model equations effectively represented the experimental data ($R^2 > 0.8$). The developed models

had also a high predictive ability (R^2 predicted > 0.8), except for TPC (R^2 pred. = 0.51). Thus, the employed factorial design effectively captured the relationship between the experimental factors and the response variables.

Aiming to obtain a soluble food ingredient from PNS insoluble matrix, maximizing the extraction of carbohydrates, while achieving the highest content of phenolic compounds and antioxidant activity under the studied conditions, the importance of carbohydrates was assigned to 10 and the remaining response factors to 1 using the Minitab v17 software program. The optimal extraction conditions established based on this approach were 180 °C, 10 min and 3 g/60 mL, obtaining a high overall desirability of $D = 0.8201$ ($0 < D < 1$) (Fig. 2). The optimal conditions had a predicted extraction yield of 16.4 %, a carbohydrate content of 335 mg/g, a TPC value of 206 mg GAE/g and an antioxidant activity of 299 mg AAE/g. The experiments validation allowed to obtain similar responses to the predicted ones ($p > 0.05$), further demonstrating the good adequacy of the developed models (**Table S4**).

As observed in Fig. 2, under the conditions used, the highest temperature results in the highest extraction of carbohydrates, phenolic compounds, and antioxidant activity, as well as yield, almost in a linear trend, from this insoluble matrix. This trend was not observed for time and m/V ratio, which showed, for all parameters, a decrease between the lowest conditions and the center points. This may be explained by the higher degradation of compounds extracted under center points conditions. However, the higher recovery of compounds with higher times and m/V ratios showed that these more extreme conditions allow to extract more compounds from the insoluble matrix than those that are degraded, as reported for brewers' spent grain (Coelho et al., 2014) and spent coffee grounds (Passos & Coimbra, 2013). This may be explained by the increase of pressure, resulting in a higher autohydrolysis due to the more acidic medium (Smith, 2002), enabling also the extraction of different polysaccharides (Passos & Coimbra, 2013; Reis et al., 2023) and phenolic compounds (Cocero et al., 2018).

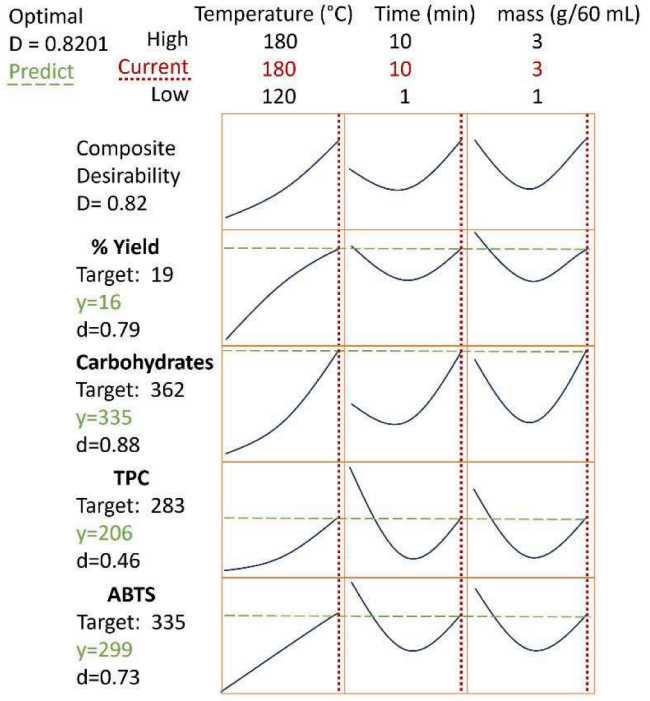

Fig. 2. Optimization plot of temperature, time, and mass/volume ratio targeting the maximization of the extraction of pine nut skin carbohydrates with the highest content of phenolic compounds and antioxidant activity.

3.2. Laboratorial scale-up of subcritical-water extraction (SWE)

To have enough material for digestion assays, a laboratorial scale-up of SWE was performed using the conditions previously optimized with PNS-F, which accounted for 85 % of the PNS sample. This scale-up was performed with PNS as a whole, skipping the sieving step, which renders an easier and cheaper utilization of this raw material. Thus, PNS was extracted at 180 °C, during 10 min, with the m/V ratio of 3 g/60 mL, while increasing the number of reactors from 2 to 8. Under these conditions, the time to reach the 180 °C was 12 min instead of the previous 2 min. In both conditions, the samples were kept at 180 °C during 10 min, with a total of 22 min of heating under the scaling-up conditions. For comparison purposes, the HWE was also scaled-up by utilizing PNS and increasing the m/V ratio to 3 g/60 mL with a total volume of 2 L.

The SWE scale-up yield, carbohydrate content, and phenolic compounds were unaltered ($p > 0.05$), while the antioxidant activity decreased from 307 to 217 mg AAE/g (Fig. 3). The scale-up of HWE (100 °C, 30 min, 3 g/60 mL), using the same m/V ratio as utilized for SWE, produced extracts with lower yield (64 %), carbohydrate content (24 %), and antioxidant activity (21 %), with an equivalent content of phenolic compounds, when compared with the scale-up of SWE. The increase of m/V ratio in HWE from 1 g/60 mL to 3 g/60 mL had a positive effect on the carbohydrate content (from 180 to 255 mg/g), a tendency previously observed for SWE when high temperatures were used (Fig. 1). This alteration, together with the use of the whole PNS, produced a 37 % decrease in antioxidant activity, and did not significantly impact the remaining responses (Fig. 3). The decrease of the antioxidant activity observed in both extraction methodologies, despite the non-significant reduction of phenolic compounds extraction, may be explained by the assay's reaction mechanisms. While the Folin–Ciocalteu assay involves a redox reaction, in which the mechanism is a single electron transfer, the ABTS assay entails the scavenging of free radicals with a mixed hydrogen atom transfer/single electron transfer reaction mechanism (Ilyasov et al., 2020). Therefore, the use of unfractionated PNS results in the extraction of phenolic compounds with lower free radical scavenging activity, that should be derived from the PNS-C (≥ 500 μm).

3.3. Carbohydrates characterization of SWE laboratorial scale-up

The extracts obtained after scale-up of SWE (PNS extracted at 180 °C, 10 min, 3 g/60 mL) and, for comparison, HWE (PNS extracted at 100 °C, 30 min, 3 g/60 mL) were fractionated according to their solubility in ethanol solutions, allowing to separate the polysaccharides, which tend to precipitate in 75 % ethanol solutions (Et75) (Nunes & Coimbra, 2002), from the free sugars, oligosaccharides, and phenolic compounds, which remain soluble in 75 % ethanol solutions (EtSn) (Coelho et al., 2014).

EtSn carbohydrates, when analyzed without hydrolysis prior to their determination as alditol acetates by GC–MS, showed to be composed by monosaccharides (12 % and 11 % for SWE and HWE, respectively) and oligosaccharides (5 %). The structured chromatogram, where compounds with lower retention time were those with lower degree of polymerization (DP) due to their higher volatility, allowed to observe DPs between 2 and 4 (Fig. 4 and Table 1). Oligosaccharides with DP higher than 5 could not be analyzed by GC-qMS, as they produce high molecular weight derivatives that are not amenable to be volatized. The quantified oligosaccharides were composed of pentoses, hexoses, or both, identified through diagnostic ions. Those at m/z 259 and m/z 303 were diagnostic for pentoses, corresponding to a non-reducing tri-acetylated pentose and to a reducing tetra-acetylated pentose, respectively, arising from the cleavage of the glycosidic bonds (**Figure S2**). The product ions arising from the glycosidic bonds cleavage of hexose-containing oligosaccharides at m/z 331 and m/z 375 were diagnostic of a non-reducing tetra-acetylated and a reducing penta-acetylated hexose residue, respectively (Silva et al., 2019). Twenty-four different disaccharides were identified for SWE and 11 for HWE. For

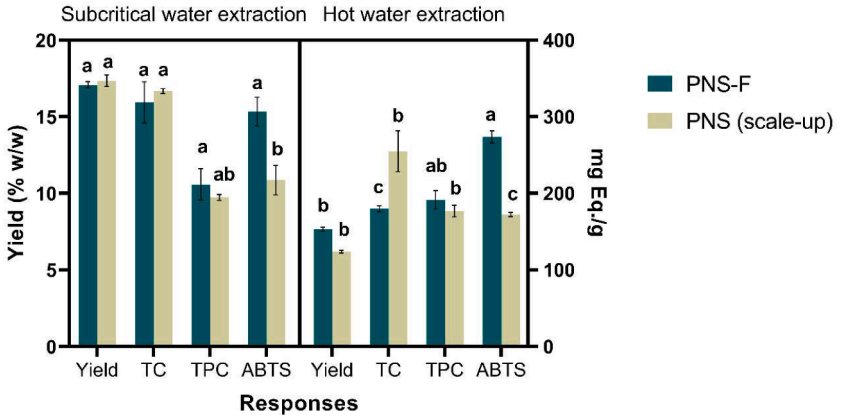

Fig. 3. Responses obtained after subcritical water extraction (SWE) of PNS-F (particle size < 500 μm) and PNS (scale-up) under the optimized conditions (180 °C, 10 min, 3 g/60 mL) and hot water extraction (HWE, 100 °C, 30 min) of PNS-F (m/V ratio of 1 g/60 mL) and PNS (scale-up, m/V ratio of 3 g/60 mL). Means of the same responses that do not share a letter are significantly different ($p < 0.05$)).

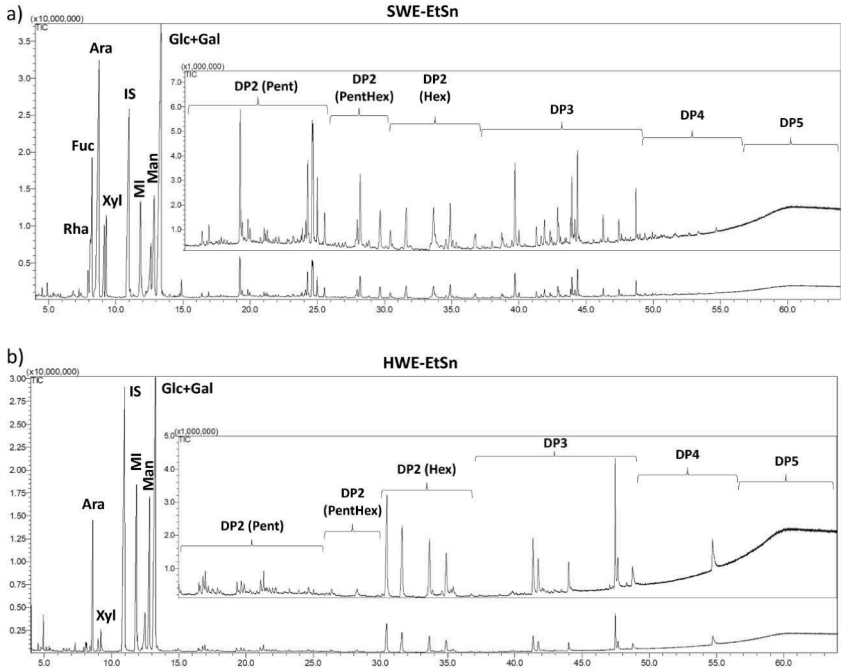

Fig. 4. GC-qMS chromatograms of oligosaccharides from SWE-EtSn (a) and HWE-EtSn (b), with magnification from 15 to 64 min. Rha – rhamnose; Fuc – fucose; Ara – arabinose; Xyl – xylose; IS – Internal standard; MI- *myo*-inositol; Man – mannose; Glc+Gal – glucose and galactose (co-elution); DP2 (Pent) – pentose disaccharides; DP2 (PentHex) – disaccharides composed of pentoses and hexoses; DP2 (Hex) – hexose disaccharides; DP3 – trisaccharides; DP4 – tetrasaccharides; DP5 – pentasaccharides.

trisaccharides, 25 were identified in SWE and 5 in HWE, and one tetrasaccharide was identified in both extracts (Fig. 4). In addition, the presence of uronic acids (UA) in the SWE-EtSn extract (34 mg/g), determined colorimetrically after hydrolysis, suggests the occurrence of pectic oligosaccharides, which were almost absent in HWE-EtSn (3.4 mg/g). *myo*-Inositol (MI) was also identified in EtSn fractions, with higher amount in HWE. These structures should arise from phosphatidylinositols, which are components of the cell membranes and consist of a glycerol backbone, two non-polar fatty acid tails, and a phosphate group substituted with an inositol polar head group (Campo & San Segundo, 2020). MI has been related to several pharmacological properties, namely the treatment of polycystic ovary syndrome, obsessive-compulsive disorder, panic disorder, depression, and neurodegenerative diseases (Derkaczew et al., 2023; López-Gambero et al., 2020).

The high-molecular weight fractions (Et75) of SWE and HWE were composed of 49 % and 45 % of polysaccharides, respectively (Table 1). Both fractions had a high content of uronic acids (140 mg/g for SWE-Et75 and 219 mg/g for HWE-Et75), galactose (97 and 62 mg/g, respectively), and arabinose (35 and 54 mg/g). Glycosidic linkage analysis (Table 2) demonstrated that 5-Ara*f* was the most abundant residue, with similar values for SWE and HWE extracts (≥ 18 %). However, after ethanol precipitation, this residue was lowered to 2.9 % in SWE-Et75, but not in HWE-Et75. This decrease was accompanied by the decrease of 3,5-Ara*f* residue by 75 %, from 4.2 % to 1.1 %. Thus, arabinans were partially degraded by SWE conditions, being recovered as monosaccharides (4 %, Table 1) and oligomers (Fig. 4) in the SWE-EtSn. The arabinans recovered by SWE had one branching point per 8 Ara*f* units, while those extracted by HWE had a lower content of branched residues (1:18), which suggests a higher depolymerization of linear arabinan chains under subcritical conditions. The occurrence of *t*-Gal*p* (7 % and 3 % for SWE-Et75 and HWE-Et75, respectively), 4-Gal*p* (4

Table 1
Yield (% w/w) and carbohydrate composition (mg/g) (monosaccharides, oligosaccharides, and *myo*-inositol in EtSn fractions and monosaccharides residues from polysaccharides in Et75 fractions) of the extracts from subcritical water extraction (SWE) and hot water extraction (HWE).

	SWE		HWE	
	EtSn	Et75	EtSn	Et75
Yield (% w/w)[a]	65	27	60	31
Rha	3.6 ± 0.1	16.9 ± 0.6	0.19 ± 0.02	10.5 ± 0.1
Fuc	9.1 ± 0.3	5.7 ± 0.2	0.55 ± 0.02	4.1 ± 0.1
Ara	39.7 ± 1.3	35.2 ± 0.4	14.8 ± 0.2	53.7 ± 2.5
Xyl	5.2 ± 0.1	56.0 ± 0.4	1.44 ± 0.03	20.7 ± 1.4
Man	12.0 ± 0.7	32.6 ± 0.2	24.7 ± 1.3	19.2 ± 0.5
Gal	19.3 ± 1.0	96.7 ± 0.6	26.4 ± 0.9	62.2 ± 0.9
Glc	29.0 ± 1.4	104.3 ± 0.8	39.7 ± 1.3	55.6 ± 1.2
UA	34.0 ± 1.0[b]	139.8 ± 7.2	3.4 ± 0.1[b]	218.7 ± 2.2
MI	16.0 ± 0.7		32.7 ± 2.1	
DP2	22.6 ± 1.3		17.6 ± 1.6	
DP3	26.9 ± 1.2		17.5 ± 1.9	
DP4	0.3 ± 0.1		7.0 ± 1.2	
Total	184 ± 6	487 ± 5	183 ± 10	445 ± 1

[a] Yield relative to the ethanol precipitation (g/100 g extract).
[b]Calculated after hydrolysis, not accounted for the total amount. Rha – rhamnose; Fuc – fucose; Ara – arabinose; Xyl – xylose; Man – mannose; Gal – galactose; Glc – glucose; UA – uronic acids; MI – myo-inositol; DP2 – disaccharides; DP3 – trisaccharides; DP4 – tetrasaccharides.

% and 8 %), and 4,6-Gal*p* (0.3 % and 1 %) suggests the presence of galactans (Table 2). The 39 % decrease of 4-Gal*p* after ethanol precipitation of SWE, not observed in HWE, indicates the depolymerization also for galactans, promoted by subcritical extraction conditions. The lower extent of hydrolysis of galactans when compared to the arabinans, observed upon SWE conditions, can be related to the lower thermal lability of galactose residues. The same trend was observed during coffee roasting with a faster depolymerization of arabinose residues from arabinogalactan side chains when compared to the galactans backbone (Simões et al., 2014).

The occurrence of 2-Rha*p* (1.6 % for SWE and 1.2 % for HWE), and 2,4-Rha*p* (1.8 % and 0.7 %, respectively), suggests the presence of type I rhamnogalacturonan (RG-I), which are linked to galacturonic acid at the *O*-2 position and are substituted at the *O*-4 position by arabinans and galactans as side chains (Fernandes et al., 2019). The abundance of 2- and 2,4-Rha*p* is similar in SWE extract and in SWE-Et75 fraction (Table 2). Thus, rhamnose-rich pectic polysaccharides backbone was preserved, on the contrary of the side chains, which were shorter due to the depletion of 5-Ara*f* and 4-Gal*p* residues. The use of high temperatures (above 160 °C) were reported to degrade RG-I side chains and homogalacturonan backbone, leading to the production of arabino-, galacto-, and pectic- oligosaccharides (Basak & Annapure, 2022). This was also observed in this study, as shown by the 10-fold increase in uronic acids (UA) content in SWE-EtSn when compared to HWE-EtSn (Table 1), and by the increased number of different oligosaccharides after SWE (Fig. 4). Thus, the degraded arabinans, galactans, and pectic polysaccharides were recovered as monomers and oligomers in the SWE-EtSn fraction (Table 1). Arabinooligosaccharides, galactooligosaccharides, and pectic oligo- and polysaccharides have all been proposed as prebiotic agents (Cantu-Jungles et al., 2021; Gerschenson, 2017; Lee et al., 2022; Mateos-Aparicio et al., 2020), as they are undigested in the gastrointestinal tract, and are capable of modulating gut microbiota by promoting the growth of short-chain fatty acids (SCFAs) producers. Pectic polysaccharides were also shown to have hypoglycemic activity, as their ingestion increases the viscosity of digesta, and may inhibit amylase activity (Bai & Gilbert, 2022), as well as anti-inflammatory and antioxidant properties (Minzanova et al., 2018).

Type II arabinogalactans (AG II) were also proposed to be extracted by both extraction conditions, as evidenced by the presence of 3-Gal*p*, 6-

Table 2
Glycosidic linkages (mol%) identified in subcritical water (SWE) and hot water (HWE) extracts before and after ethanol precipitation (Et75). Residues with values < 0.1 % for all samples were removed.

Glycosyl linkage	SWE	SWE-Et75	HWE	HWE-Et75
t-Rha*p*	0.7	0.9	0.9	1.1
2-Rha*p*	1.6	2.0	1.2	1.2
2,4-Rha*p*	1.8	2.3	0.7	1.1
Total	**4.1 (4)**	**5.1 (4)**	**2.8 (2)**	**3.4 (3)**
t-Fuc*p*	0.9	1.0	1.0	1.0
Total	**0.9 (2)**	**1.0 (1)**	**1.0 (1)**	**1.0 (1)**
t-Ara*f*	8.4	3.1	5.8	4.3
3-Ara*f*	3.5	1.3	2.7	1.7
5-Ara*f*	18.4	2.9	27.2	22.9
3,5-Ara*f*	4.2	1.1	2.9	1.7
Total	**34.5 (29)**	**8.4 (10)**	**38.6 (20)**	**30.6 (15)**
t-Xyl*p*	7.8	9.8	6.1	6.7
2-Xyl*p*	3.5	5.5	2.1	3.5
4-Xyl*p*	3.1	4.3	1.0	3.5
2,4-Xyl*p*	3.1	2.2	2.6	5.0
Total	**17.5 (8)**	**21.8 (15)**	**11.8 (4)**	**18.8 (6)**
t-Man*p*	0.4	0.5	0.4	0.3
4-Man*p*	2.1	1.9	2.1	2.2
6-Man*p*	0.3	0.4	0.7	0.5
4,6-Man*p*	0.5	0.7	0.2	0.5
Total	**3.3 (5)**	**3.5 (7)**	**3.5 (6)**	**3.5 (4)**
t-Gal*p*	4.5	7.1	3.1	2.7
2-Gal*p*	0.9	1.5	1.6	1.1
3-Gal*p*	1.5	9.5	1.3	2.0
4-Gal*p*	6.5	3.9	4.6	8.1
6-Gal*p*	1.2	2.1	0.8	0.8
3,6-Gal*p*	1.6	2.9	1.9	2.8
4,6-Gal*p*	0.3	0.3	0.7	1.0
Total	**16.4 (16)**	**27.3 (22)**	**14.1 (19)**	**18.5 (14)**
t-Glc*p*	1.8	1.5	9.6	3.0
3-Glc*p*	3.9	6.0	2.2	5.3
4-Glc*p*	3.5	4.2	1.9	1.8
6-Glc*p*	0.8	1.4	2.6	0.8
2,6-Glc*p*	0.1	0.2	2.0	0.4
3,4-Glc*p*	0.2	0.3	0.5	0.6
4,6-Glc*p*	11.3	17.7	4.8	8.6
3,4,6-Glc*p*	0.3	0.5	1.3	0.7
Total	**21.9 (19)**	**31.7 (23)**	**24.9 (26)**	**21.3 (12)**
Pectic polysaccharides (% w/w)		**47**		**71**
Type II AGs (% w/w)		**11**		**4**
XG (% w/w)		**24**		**11**

Values between parentheses represent the mol% of each monomer quantified as alditol acetates. The amount of each monomer corresponding to the glycosidic linkages attributed to each polysaccharide, was employed to determine the percentages of pectic polysaccharides (2- and 2,4-Rha*p*; 100 % Ara; *t*-, 4- and 4,6-Gal*p*; 100 % UA), type II AGs (3-, 6-, and 3,6-Gal*p*) and XG (100 % Fuc; *t*- and 2-Xyl*p; t*-, 4-, 4,6-Glc*p*; 2-Gal*p*).

Gal*p*, and 3,6-Gal*p*, especially in SWE-Et75, where they accounted for 14 % of the identified glycosidic residues, compared with 6 % in HWE-Et75 (Table 2). These polysaccharides are known to be usually linked to proteins (arabinogalactan proteins, AGP) or RG-I side chains (Ghosh et al., 2023). The occurrence of *t*-Rha*p*, characteristic of AGP, reported to be linked to the *O*-5 of Ara*f* (Hamed et al., 2022; Nunes et al., 2008), reinforce the presence of these polysaccharides. AG II were also extracted from pistachio hull, and exhibited immune-enhancing effects (Hamed et al., 2022).

The high abundance of 4,6-Glc*p* (17.7 % and 8.6 % for SWE-Et75 and HWE-Et75, respectively), together with 4-Glc*p* (4.2 % and 1.8 %), *t*-Xyl*p* (9.8 % and 6.7 %), 2-Xyl*p* (5.5 % and 3.5 %), 2-Gal*p* (1.5 % and 1.1 %), and *t*-Fuc*p* (1.0 % for both) (Table 2), indicates the presence of xyloglucans (XG) (Fernandes et al., 2019). The relative proportion of this polysaccharide had a 2-fold increase from the hot water to the

subcritical water extract (11–24 %), as observed by the amount of xylose (21 mg/g and 56 mg/g, respectively) and glucose (56 mg/g and 104 mg/g) in each ethanol precipitated fraction (Table 1). XG extracted by both SWE and HWE were found to be highly substituted, with branching degrees (calculated as the ratio % between 4,6-Glc*p* and the sum of *t*-, 4-, and 4,6-Glc*p*) of 76 % and 65 %, respectively. This level of branching is consistent with what is typically observed in other species, where there is one unsubstituted unit per every 4 Glc*p* units (Tuomivaara et al., 2015). Considering the mol% of *t*-Xyl*p* as the terminals of XG side chains, Glc*p* substituted at *O*-6 by α-D-Xyl*p* explains about 60 % of the branching points (Table 2). The other possible side chain structures found in gymnosperms (Tuomivaara et al., 2015), namely Xyl*p* substituted at *O*-2 by β-D-Gal*p* and Gal*p* substituted at *O*-2 by α-L-Fuc*p*, are composed by a residue of 2-Xyl*p*, explaining the remaining 40 % of branching. Based on the mol% of *t*-Fuc*p*, it was inferred a substitution with Fuc*p* residues of about 5 % and 11 % of XG for SWE and HWE, respectively. Thus, the remaining 35 % and 29 % branching structures were composed of terminally linked galactose, linked to xylose at the *O*-2 position.

XG consumption has been reported to protect from mucosal disruption diseases, being able to alleviate symptoms of gastroenteritis, nasal disorders, and dry eye syndrome (Piqué et al., 2018). These polysaccharides are also considered as fiber, reaching the colon intact. Their fermentation led to SCFAs production (Cantu-Jungles et al., 2019), improved the microbial profile of high-fat mice and increased the bile acids excretion, proposing them as prebiotic and hypolipidemic agents (Cheng et al., 2020).

3.4. Characterization of phenolic compounds from pine nut skin

To characterize the phenolic compounds in the free and soluble-bound form, pine nut skin was sequentially extracted with organic solvents, yielding a total of 14.3 mg GAE/g PNS, and the resultant residue was alkaline extracted to release the esterified compounds from the insoluble-bound compounds (32.6 mg GAE/g PNS). The total amount given by the sum of the two forms was 46.8 mg GAE/g PNS (Fig. 5). The insoluble-bound phenolic compounds occur covalently linked to cell-wall structures, through ester, ether, and C–C bonds (Acosta-Estrada et al., 2014). Alkaline hydrolysis allows to recover ester-linked phenolic compounds. Therefore, the ether and C–C linked were not quantified.

Subcritical water extraction (SWE, PNS extracted at 180 °C, 10 min, 3 g/60 mL) allowed to recover 29 % of the insoluble-bound phenolic compounds in addition to the free and soluble-bound (24 mg GAE/g PNS), when compared to the total extractable by sequential organic solvents and alkaline hydrolysis (Fig. 5). The hot water extraction (HWE, PNS extracted at 100 °C, 30 min, 3 g/60 mL) allowed to obtain only 54 % of the free and soluble-bound phenolic compounds, resulting in 7.7 mg GAE/g PNS. The use of SWE conditions enabled the cleavage of bound phenolic compounds, as observed by the higher recovery of phenolic compounds than with organic solvents.

From the identified phenolic compounds obtained by organic solvents and aqueous alkaline extractions (Table 3), *p*-hydroxybenzaldehyde, protocatechuic, gallic, *p*-coumaric, vanillic, and ferulic acids were identified and quantified on the SWE and HWE extracts (Table 4). Protocatechuic acid was the most abundant compound in both extracts (2129 and 2905 μg/g for SWE-EtSn and HWE-EtSn, respectively). The use of SWE enabled to recover 2-fold of protocatechuic acid from PNS when compared to HWE (235 and 105 μg/g PNS, respectively). Gallic acid was the second most abundant in both extracts (475 μg/g for SWE-EtSn and 575 μg/g for HWE-EtSn), and it was 2.5-fold more extracted from PNS when using SWE (53 μg/g PNS) when compared to HWE (21 μg/g PNS). The extraction in free *p*-hydroxybenzaldehyde (2.3 and 0.4 μg/g PNS for SWE and HWE, respectively) and vanillin (4 and 1 μg/g PNS, respectively) was higher in SWE conditions than in HWE (Table 4), which should be resultant from the partial degradation of lignin under subcritical conditions (Fache et al., 2016).

After alkaline hydrolysis of PNS-C residue, vanillic, caffeic, *p*-coumaric, and ferulic acids were observed to be linked to the 10,16-dihydroxyhexadecanoic acid (Table 3 **and Figure S3**), showing an incomplete de-esterification. This long-chain fatty acid is known to be a cutin monomer, esterified to glycerol, and can be bound to hydroxycinnamic acids, namely caffeic, ferulic, and coumaric acids (Kong et al., 2020). Cutin can only be partially solubilized in alkaline medium (Razeq et al., 2021), which explains the observation of 10,16-dihydroxyhexadecanoic acid both free and esterified with phenolic acids. It has been shown that monomers of 10,16-dihydroxyhexadecanoic acid can be polymerized through the terminal (resulting in a linear structure) or the midchain hydroxyl group (resulting in a branched structure) (Reynoud et al., 2021). However, the precise position of the ester-linked phenolic compounds within the structure of cutin has not yet been established. Thus, phenolics esterification may occur at the terminal or midchain position (**Figure S3**). The lower amounts of vanillic, *p*-coumaric, and ferulic acids in the free form (Table 4) after SWE, when compared to HWE, could be resultant from their thermal degradation or reaction with other compounds during the extraction process (Antony & Farid, 2022). The absence of caffeic acid on both SWE and HWE extracts (Table 4), along with the lower amount of the remaining phenolics esterified to 10, 16-dihydroxyhexadecanoic acid in SWE, indicates that cutin structures are stable under subcritical conditions, as the compounds linked to the fatty acids were not released to their free form.

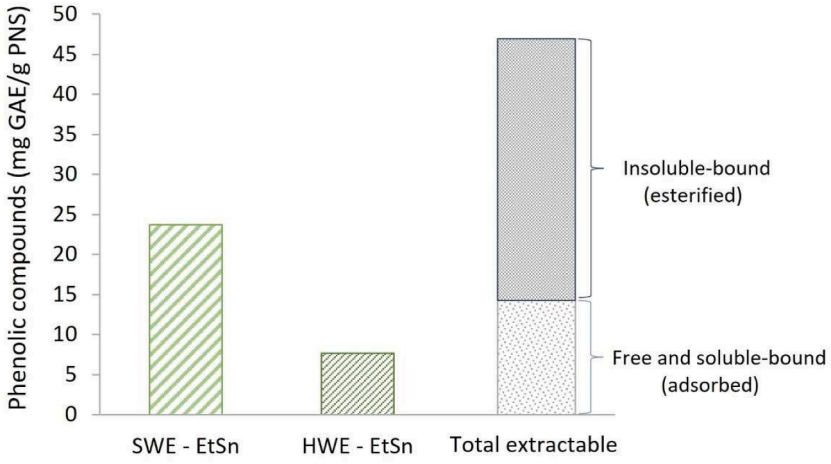

Fig. 5. Quantification of total phenolic compounds (mg GAE/g pine nut skin) of low-molecular weight fractions (EtSn) obtained by subcritical water (SWE) and hot water (HWE) extractions, and free and soluble-bound compounds extracted by organic solvents, and insoluble-bound compounds obtained after alkaline hydrolysis.

Table 3
Tentative identification of phenolic compounds, lipophilic compounds, and phenolic derivatives obtained by sequential extraction with organic solvents (free form) and alkaline hydrolysis (insoluble-bound form) by HPLC-DAD/ESI-MS, corresponding fragmentation pattern and mass errors (Δ ppm).

Compound tentative identification	Molec. formula	$[M-H]^-$ obs.	MS^2 (*m/z*)	Δ ppm	Free	Insoluble bound
Phenolic compounds						
p-Hydroxybenzaldehyde	$C_7H_6O_2$	121.029	92	1.034	✓	
Guaiacol	$C_7H_8O_2$	123.045	81	1.064		✓
3-Methylbenzoic acid*	$C_8H_8O_2$	135.045	134; 91	1.034	✓	✓
p-Hydroxybenzoic acid	$C_7H_6O_3$	137.024	93	1.049	✓	
Protocatechuic acid	$C_7H_6O_4$	153.019	109	0.995	✓	✓
p-Coumaric acid	$C_9H_8O_3$	163.040	119	1.069	✓	✓
Vanillic acid	$C_8H_8O_4$	167.035	152; 123; 108	1.135	✓	✓
Gallic acid	$C_7H_6O_5$	168.989		23.690	✓	✓
Caffeic acid	$C_9H_8O_4$	179.035	135	0.855		✓
3,4-Dihydroxymandelic acid	$C_8H_8O_5$	183.030	139; 121; 97	0.852	✓	✓
Ferulic acid	$C_{10}H_{10}O_4$	193.051	178; 134	0.616	✓	✓
Carboxyvanillic acid	$C_9H_8O_6$	211.025	123; 81	1.006		✓
Lipophilic compounds						
Azelaic acid	$C_9H_{16}O_4$	187.098	125; 97	0.566	✓	✓
10,16-Dihydroxyhexadecanoic acid	$C_{16}H_{32}O_4$	287.223	269	0.784		✓
7-Hydroxyhexadecanedioic acid	$C_{16}H_{30}O_5$	301.202	283; 265; 221	0.860		✓
Aleuritic acid	$C_{16}H_{32}O_5$	303.217	285; 267	0.619		✓
Phenolic derivatives						✓
Coumaroyl-hydroxyhexadecanoic acid	$C_{25}H_{38}O_6$	433.259	287; 163; 145; 119	0.300		✓
Caffeoyl-hydroxyhexadecanoic acid	$C_{25}H_{38}O_7$	449.254	287; 179; 161; 135	0.700		✓
Feruloyl-hydroxyhexadecanoic acid	$C_{26}H_{40}O_7$	463.270	431; 287; 193; 175; 134	0.700		✓
Vanilloyl-hydroxyhexadecanoic acid	$C_{25}H_{38}O_9$	481.244	287; 167; 149; 123	0.931		✓
Caffeoyl-pinellic acid	$C_{27}H_{40}O_8$	491.265	473; 449; 179; 161; 135	0.400		✓
Caffeoyl-hexadecyl-dihydroxyhexadecanoic acid	$C_{42}H_{72}O_{10}$	719.473	449; 431; 287; 179; 161; 135			✓

Table 4
Identification and quantification (μg/g of extract and μg/g of pine nut skin) of the phenolic compounds present in the low-molecular weight (EtSn) pine nut skin extracts obtained by subcritical water (SWE) and hot water (HWE) extractions, by HPLC-ESI-MS.

Identified compound	$[M-H]^-$ (*m/z*)	MS^2 (*m/z*)	SWE (μg/g)	HWE (μg/g)	SWE (μg/g PNS)	HWE (μg/g PNS)
p-Hydroxybenzaldehyde	121	92	21.2	12.3	2.3	0.4
p-Hydroxybenzoic acid	137	93	6.3	14.9	0.7	0.5
Vanillin	151	136; 108	36.5	27.1	4.0	1.0
Protocatechuic acid	153	109	2128.7	2904.7	235.2	104.6
p-Coumaric acid	163	119; 93	2.6	13.2	0.3	0.5
Vanillic acid	167	152; 123; 108	39.9	235.3	4.4	8.5
Gallic acid	169	125; 79	475.1	575.4	52.5	20.7
Ferulic acid	193	178; 134	1.1	5.1	0.1	0.2
Catechin	289	245; 123	0.9	18.8	0.1	0.7
Epicatechin	289	245; 203	6.1	2.5	0.7	0.1
Quercetin	301	150; 121	1.9	0.5	0.2	0.0
Rutin	609	300; 271	0.0	0.6	0.00[a]	0.02[a]
Total			2724.0	3831.1	301.0	137.9

Means without a superscript are significantly different ($p < 0.05$), Statistical significance determined using the Holm–Sidak method ($\alpha = 0.05$). Standards of previously identified 3,4-dihydroxymandelic acid, carboxyvanillic acid and guaiacol were not available for quantification .

Proanthocyanidins were also identified after organic solvent and SWE and HWE. After purification (Sephadex LH-20) and acidic hydrolysis, it was possible to determine the presence of procyanidins composed of monomers of epicatechin and/or catechin (**Figure S4**). The total amount obtained after the sequential extractions, estimated as catechin equivalents (CE), was 9 mg CE/g PNS, 14 mg CE/g PNS for SWE, and 5 mg CE/g PNS for HWE (**Figure S4**). The enhanced extractability of these compounds through SWE can be attributed to the higher temperatures achieved, which facilitated the penetration of water into the matrix (de Hoyos-Martínez et al., 2019). The increase in epicatechin content from HWE to SWE (0.1–0.7 μg/g PNS) (Table 4) may be attributed to the depolymerization of procyanidins under high temperatures (Li et al., 2015).

3.5. Stability of SWE and HWE extracts throughout the gastrointestinal digestion

The reported prebiotic effects of oligo- and polysaccharides only occurs if they are stable throughout the digestion process, maintaining their structural integrity as they reach the colon. Among the enzymes present along the gastrointestinal tract, only amylase (oral and intestinal phases) possesses the capability to hydrolyze starch and related carbohydrates containing three or more (1→4)-α-linked D-glucose units (Fischer & Stein, 1960). In addition to enzymatic activity, the acidic stomach media (pH around 3) along with the 2 h residence time may promote the hydrolysis of the linkages between the compounds' monomers (Bornhorst & Singh, 2012).

Free carbohydrates of EtSn fractions from SWE and HWE were quantified in the initial samples and after undergoing digestion, in the oral, gastric, and intestinal phases. Regarding the mono- and oligosaccharides present in the low-molecular weight (EtSn) fractions obtained from SWE and HWE, no significant differences were observed between the initial samples and the intestinal phase (**Figure S5**). Thus, mono- and oligosaccharides stability was not affected by the digestion conditions. Regarding the Et75 fractions, the initial SWE and HWE extracts contained 0.8 % and 1 % of free sugars and *myo*-inositol, respectively (**Figure S6**). After digestion, there was a significant increase in galactose, glucose, and *myo*-inositol levels in both SWE-Et75 and HWE-Et75

fractions, although resulting only in a 1 % increase. The release of *myo*-inositol upon intestinal conditions is likely due to the action of pancreatin lipases on phosphatidylinositols. The low release of glucose and galactose (0.2–0.4 %) allows to infer that the polysaccharides of both water extraction methods, namely pectic, XG, and AG II were not affected by the digestion process. These soluble polysaccharides need to remain intact as they reach the colon, to be fermented by the microbiota, thus acting as functional prebiotic substrates.

Regarding phenolic compounds, the digestion process produced a 23 % decrease in total phenolic compounds from the initial SWE-EtSn extract to the intestinal phase, while it did not significantly affect their content in HWE-EtSn (Fig. 6a). Regarding the antioxidant activity, it was observed a 28 % and 20 % reduction for SWE and HWE, respectively, after the intestinal conditions (Fig. 6b). The higher impact of intestinal conditions on the phenolic compounds content and antioxidant activity, compared to the remaining digestion phases, was extensively observed in various *in vitro* gastrointestinal digestion studies (Cuvas-Limon et al., 2022; Gómez-Mejía et al., 2022; Seraglio et al., 2017). This higher instability may be justified from the neutral pH value in the intestinal environment, which exceeds the pKa of the phenolic compounds, leading to their deprotonation. Therefore, epimerization and auto-oxidation reactions are promoted (Gómez-Mejía et al., 2022; Pant et al., 2019), decreasing the phenolic compounds capacity to reduce Folin–Ciocalteu reagent and scavenge free radical $ABTS^{\bullet+}$. Consequently, this results in a decrease in the measured amount of phenolic compounds and their antioxidant activity.

As the phenolic compounds and respective antioxidant activity were only affected by the intestinal conditions, the individual quantification was performed at this phase (Fig. 6c). The free phenolic compounds from SWE-EtSn and HWE-EtSn displayed distinct behavior within the intestinal environment. For SWE, *p*-hydroxybenzaldehyde and vanillic, *p*-hydroxybenzoic and ferulic acids increased significantly (ranging from 35 to 139 % increase) from the initial to the intestinal phase, while the remaining were not significantly affected. Ferulic acid, which exhibited the highest increase (2.3-fold) after intestinal digestion of SWE-EtSn (Fig. 6c), was reported to occur ester-linked to primary cell walls in

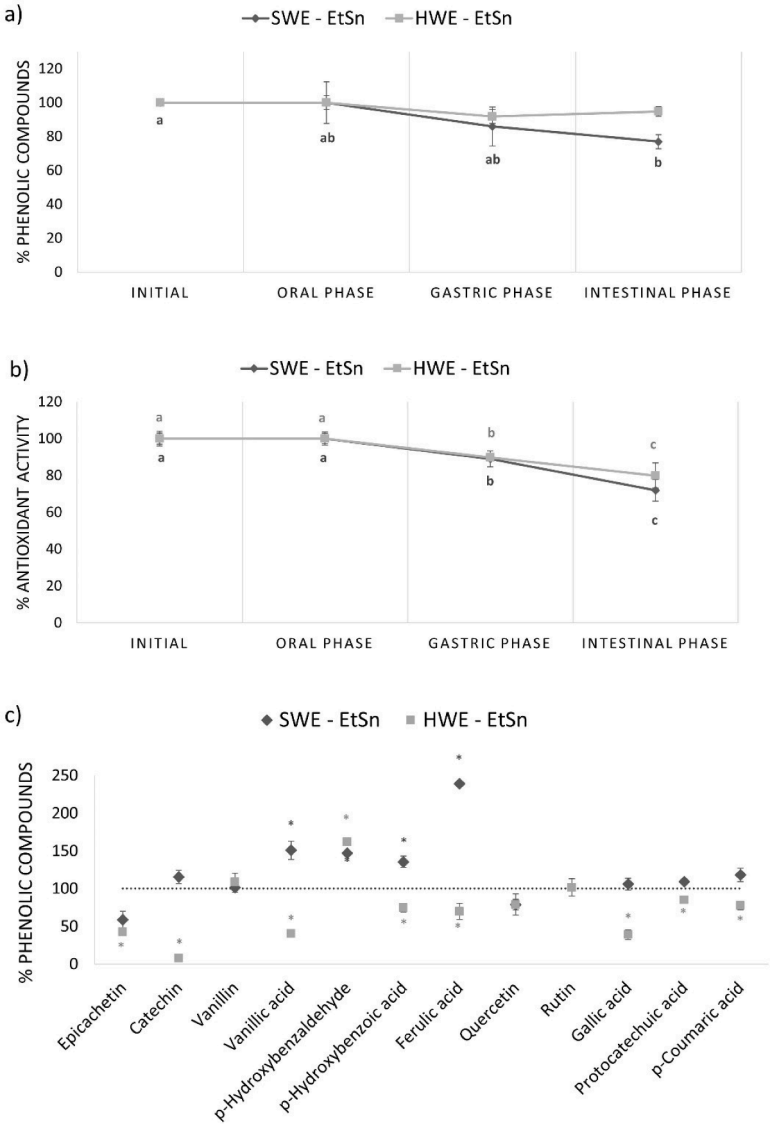

Fig. 6. Impact of digestion on the phenolic compounds and antioxidant activity of the low-molecular weight fractions (EtSn) from subcritical water (SWE) and hot water (HWE) extractions. Relative percentages of (a) phenolic compounds (gallic acid equivalents) and (b) antioxidant activity (ABTS assay, ascorbic acid equivalents) in each *in vitro* digestion phase (oral, gastric, and intestinal). Statistical significance obtained by two-way ANOVA and Tukey post-hoc test ($p < 0.05$), samples with the same superscript are not statistically different. (c) Quantified phenolic compounds in the intestinal phase, by LC–MS^n. Statistical significance determined using the Holm–Sidak method ($\alpha = 0.05$) by comparing the initial and the intestinal phase amounts (μg/g) of each compound, statistically different means are marked with an (*).

gymnosperms (Carnachan & Harris, 2000). The increase or maintenance of phenolic compounds from SWE could potentially be explained by the presence of compounds with higher molecular weight, which may undergo cleavage during digestion, releasing the linked phenolic compounds that became bioaccessible. In the case of HWE, most of the identified compounds either decreased or remained stable, except for *p*-hydroxybenzaldehyde that suffered a 62 % increase. The decrease in the quantified phenolic compounds in HWE could be related to the presence of only free and soluble bound forms (Fig. 5) that are susceptible to the abovementioned reactions.

4. Conclusion

Pine nut skin (PNS) can be extracted by using hot water with or without pressure (up to 55 bar), namely subcritical (SWE) and hot water (HWE) extraction, producing extracts rich in soluble fiber and phenolic compounds. The use of SWE (180 °C, 10 min, 3 g PNS/60 mL water) enabled to attain higher extraction yields, and extracts with a higher content of XG, pectic oligosaccharides, and phenolic compounds with antioxidant activity. SWE demonstrated the ability to extract phenolic compounds that were bound to the cell wall, as evidenced by the recovery of higher amounts (24 mg GAE/g PNS) compared to those in the free and soluble-bound forms (14.3 mg GAE/g PNS). The release of free phenolic compounds after *in vitro* digestion of SWE-EtSn indicates the presence of oligomers containing phenolic compounds, which undergo cleavage, increasing their bioaccessibility. Oligo- and polysaccharides structures proved to be stable during the gastrointestinal digestion process, being able to reach the colon intact, where they can be selectively metabolized by healthy gut microbiota, promoting a prebiotic effect on the host

As future perspective, the suitability of subcritical water extraction as a valorization tool of pine nut skin, will be used to produce extracts rich in pectic polysaccharides, xyloglucans, and phenolic compounds to be used as food ingredients.

Funding

This work was financially supported by the Research Unit LAQV/REQUIMTE (LA/P/0008/2020 DOI 10.54499/LA/P/0008/2020, UIDB/50006/2020 DOI 10.54499/UIDB/50006/2020, and UIDP/50006/2020 DOI 10.54499/UIDP/50006/2020) through national funds and, where applicable, co-financed by FEDER, within the PT2020 Partnership Agreement, as well as by the strategic funding of UIDB/04469/2020 unit, and by LABBELS – Associate Laboratory in Biotechnology, Bioengineering, and Microelectromechanical Systems, LA/P/0029/2020. Soraia P. Silva and Abigail González acknowledge FCT for the Ph.D. grants (SFRH/BD/136471/2018 and 2021.06268.BD, respectively). Elisabete Coelho thanks the research contract (CDL-CTTRI-88-ARH/2018 – REF. 049-88-ARH/2018) funded by national funds (OE), through FCT, in the scope of the framework contract foreseen in the numbers 4, 5 and 6 of the article 23, of the Decree-Law 57/2016, of August 29, changed by Law 57/2017, of July 19. Pedro Ferreira-Santos would like to express gratitude to the Spanish Ministry of Science, Innovation and Universities and the European Union - NextGenerationEU/PRTR - for financial support (FJC2021-046978-I). Clarisse Nobre acknowledges FCT for the Assistant Research Contract (DOI 10.54499/2021.01234.CEECIND/CP1664/CT0019).

CRediT authorship contribution statement

Soraia P. Silva: Writing – original draft, Visualization, Validation, Methodology, Investigation, Formal analysis, Conceptualization. **Pedro Ferreira-Santos:** Writing – review & editing, Investigation. **Guido R. Lopes:** Writing – review & editing, Methodology, Investigation. **Sofia F. Reis:** Writing – review & editing, Investigation. **Abigail González:** Writing – review & editing, Investigation. **Clarisse Nobre:** Writing – review & editing, Resources. **Victor Freitas:** Writing – review & editing, Resources. **Manuel A. Coimbra:** Writing – review & editing, Validation, Supervision, Resources, Project administration, Investigation, Funding acquisition, Conceptualization. **Elisabete Coelho:** Writing – review & editing, Validation, Supervision, Resources, Project administration, Investigation, Funding acquisition, Conceptualization.

Declaration of competing interest

The authors declare that they have no known competing financial interests or personal relationships that could have appeared to influence the work reported in this paper.

Data availability

Data will be made available on request.

Supplementary materials

Supplementary material associated with this article can be found, in the online version, at doi:10.1016/j.carpta.2024.100508.

References

Acosta-Estrada, B. A., Gutiérrez-Uribe, J. A., & Serna-Saldívar, S. O. (2014). Bound phenolics in foods, a review. *Food Chemistry, 152*, 46–55. https://doi.org/10.1016/j.foodchem.2013.11.093

Adelina, N. M., Wang, H., Zhang, L., Yang, K., Zhang, L., & Zhao, Y. (2022). Evaluation of roasting conditions as an attempt to improve bioactive compounds and antioxidant activities of pine nut shell and skin. *Waste and Biomass Valorization, 13*, 845–861. https://doi.org/10.1007/s12649-021-01589-6

Añibarro-Ortega, M., Pinela, J., Barros, L., Ćirić, A., Silva, S. P., Coelho, E., Mocan, A., Calhelha, R. C., Soković, M., Coimbra, M. A., & Ferreira, I. C. F. R. (2019). Compositional features and bioactive properties of *Aloe vera* leaf (Fillet, Mucilage, and Rind) and flower. *Antioxidants, 8*(10), 444. https://doi.org/10.3390/antiox8100444

Antony, A., & Farid, M. (2022). Effect of temperatures on polyphenols during extraction. *Applied Sciences, 12*(4), 2107. https://doi.org/10.3390/app12042107

Bai, Y., & Gilbert, R. G. (2022). Mechanistic understanding of the effects of pectin on *in vivo* starch digestion: A review. *Nutrients, 14*(23), 5107. https://doi.org/10.3390/nu14235107

Basak, S., & Annapure, U. S. (2022). The potential of subcritical water as a "green" method for the extraction and modification of pectin: A critical review. *Food Research International, 161*, Article 111849. https://doi.org/10.1016/j.foodres.2022.111849

Bornhorst, G. M., & Singh, R. P. (2012). Bolus formation and disintegration during digestion of food carbohydrates. *Comprehensive Reviews in Food Science and Food Safety, 11*(2), 101–118. https://doi.org/10.1111/j.1541-4337.2011.00172.x

Brodkorb, A., Egger, L., Alminger, M., Alvito, P., Assunção, R., Ballance, S., Bohn, T., Bourlieu-Lacanal, C., Boutrou, R., Carrière, F., Clemente, A., Corredig, M., Dupont, D., Dufour, C., Edwards, C., Golding, M., Karakaya, S., Kirkhus, B., Le Feunteun, S., … Recio, I. (2019). INFOGEST static *in vitro* simulation of gastrointestinal food digestion. *Nature Protocols, 14*(4), 991–1014. https://doi.org/10.1038/s41596-018-0119-1

Campo, S., & San Segundo, B. (2020). Systemic induction of phosphatidylinositol-based signaling in leaves of arbuscular mycorrhizal rice plants. *Scientific Reports, 10*(1), 1–17. https://doi.org/10.1038/s41598-020-72985-6

Cantu-Jungles, T. M., do Nascimento, G. E., Zhang, X., Iacomini, M., Cordeiro, L. M. C., & Hamaker, B. R. (2019). Soluble xyloglucan generates bigger bacterial community shifts than pectic polymers during *in vitro* fecal fermentation. *Carbohydrate Polymers, 206*, 389–395. https://doi.org/10.1016/j.carbpol.2018.11.011

Cantu-Jungles, T. M., Zhang, X., Kazem, A. E., Iacomini, M., Hamaker, B. R., & Cordeiro, L. M. C. (2021). Microwave treatment enhances human gut microbiota fermentability of isolated insoluble dietary fibers. *Food Research International, 143*, Article 110293. https://doi.org/10.1016/j.foodres.2021.110293

Carnachan, S. M., & Harris, P. J. (2000). Ferulic acid is bound to the primary cell walls of all gymnosperm families. *Biochemical Systematics and Ecology, 28*(9), 865–879. https://doi.org/10.1016/S0305-1978(00)00009-0

Cheng, J., Jiang, X., Li, J., Zhou, S., Bai, T., Qin, W., Li, H., Luo, Y., Huang, Z., Liu, Y., Wu, D., Yu, B., Chen, D., & Chen, H. (2020). Xyloglucan affects gut-liver circulating bile acid metabolism to improve liver damage in mice fed with high-fat diet. *Journal of Functional Foods, 64*, Article 103651. https://doi.org/10.1016/j.jff.2019.103651

Cocero, M. J., Cabeza, Á., Abad, N., Adamovic, T., Vaquerizo, L., Martínez, C. M., & Pazo-Cepeda, M. V. (2018). Understanding biomass fractionation in subcritical & supercritical water. *The Journal of Supercritical Fluids, 133*, 550–565. https://doi.org/10.1016/j.supflu.2017.08.012

Coelho, E., Rocha, M. A. M., Saraiva, J. A., & Coimbra, M. A. (2014). Microwave superheated water and dilute alkali extraction of brewers' spent grain arabinoxylans and arabinoxylo-oligosaccharides. *Carbohydrate Polymers, 99*, 415–422. https://doi.org/10.1016/j.carbpol.2013.09.003

Coimbra, M. A., Delgadillo, I., Waldron, K. W., & Selvendran, R. R. (1996). Isolation and analysis of cell wall polymers from olive pulp. In *Modern methods of plant analysis, 17* pp. 19–44). Berlin Heidelberg: Springer. https://doi.org/10.1007/978-3-642-60989-3_2

Cruz, M. G., Bastos, R., Pinto, M., Ferreira, J. M., Santos, J. F., Wessel, D. F., … Coimbra, M. A. (2018). Waste mitigation: From an effluent of apple juice concentrate industry to a valuable ingredient for food and feed applications. *Journal of Cleaner Production, 193*, 652–660. https://doi.org/10.1016/j.jclepro.2018.05.109

Cuvas-Limon, R. B., Ferreira-Santos, P., Cruz, M., Teixeira, J. A., Belmares, R., & Nobre, C. (2022). Effect of gastrointestinal digestion on the bioaccessibility of phenolic compounds and antioxidant activity of fermented *Aloe vera* juices. *Antioxidants, 11*(12), 2479. https://doi.org/10.3390/antiox11122479

de Hoyos-Martínez, P. L., Merle, J., Labidi, J., & Charrier-El Bouhtoury, F. (2019). Tannins extraction: A key point for their valorization and cleaner production. *Journal of Cleaner Production, 206*, 1138–1155. https://doi.org/10.1016/j.jclepro.2018.09.243

Del-Castillo-Llamosas, A., Eibes, G., Ferreira-Santos, P., Pérez-Pérez, A., Del-Río, P. G., & Gullón, B. (2023). Microwave-assisted autohydrolysis of avocado seed for the recovery of antioxidant phenolics and glucose. *Bioresource Technology, 385*, Article 129432. https://doi.org/10.1016/j.biortech.2023.129432

Derkaczew, M., Martyniuk, P., Osowski, A., & Wojtkiewicz, J. (2023). Cyclitols: From basic understanding to their association with neurodegeneration. *Nutrients, 15*(9), 2029. https://doi.org/10.3390/nu15092029

DuBois, M., Gilles, K. A., Hamilton, J. K., Rebers, P. A., & Smith, F. (1956). Colorimetric method for determination of sugars and related substances. *Analytical Chemistry, 28*(3), 350–356. https://doi.org/10.1021/ac60111a017

Erşan, S., Güçlü Üstündağ, Ö., Carle, R., & Schweiggert, R. M. (2018). Subcritical water extraction of phenolic and antioxidant constituents from pistachio (*Pistacia vera* L.) hulls. *Food Chemistry, 253*, 46–54. https://doi.org/10.1016/j.foodchem.2018.01.116

Fache, M., Boutevin, B., & Caillol, S. (2016). Vanillin production from lignin and its use as a renewable chemical. *ACS Sustainable Chemistry and Engineering, 4*(1), 35–46. https://doi.org/10.1021/acssuschemeng.5b01344

Fernandes, P. A. R., Silva, A. M. S., Evtuguin, D. V., Nunes, F. M., Wessel, D. F., Cardoso, S. M., & Coimbra, M. A. (2019). The hydrophobic polysaccharides of apple pomace. *Carbohydrate Polymers, 223*, Article 115132. https://doi.org/10.1016/j.carbpol.2019.115132

Ferreira-Santos, P., Nobre, C., Rodrigues, R. M., Genisheva, Z., Botelho, C., & Teixeira, J. A. (2024). Extraction of phenolic compounds from grape pomace using ohmic heating: Chemical composition, bioactivity and bioaccessibility. *Food Chemistry, 436*, Article 137780. https://doi.org/10.1016/j.foodchem.2023.137780

Fischer, E.H., Stein, E.A. (1960). KEGG enzyme: 3.2.1.1. The Enzymes, 2nd Ed. https://www.genome.jp/entry/3.2.1.1.

Gerschenson, L. N. (2017). The production of galacturonic acid enriched fractions and their functionality. *Food Hydrocolloids, 68*, 23–30. https://doi.org/10.1016/j.foodhyd.2016.11.030

Ghosh, K., Takahashi, D., & Kotake, T. (2023). Plant type II arabinogalactan: Structural features and modification to increase functionality. *Carbohydrate Research, 529*, Article 108828. https://doi.org/10.1016/j.carres.2023.108828

Gómez-Mejía, E., Rosales-Conrado, N., León-González, M. E., Valverde, A., & Madrid, Y. (2022). A combined analytical-chemometric approach for the *in vitro* determination of polyphenol bioaccessibility by simulated gastrointestinal digestion. *Analytical and Bioanalytical Chemistry, 414*(8), 2739–2755. https://doi.org/10.1007/s00216-022-03922-x

Gudiña, E. J., Couto, M. R., Silva, S. P., Coelho, E., Coimbra, M. A., Teixeira, J. A., & Rodrigues, L. R. (2022). Sustainable exopolysaccharide production by *Rhizobium viscosum* CECT908 using corn steep liquor and sugarcane molasses as sole substrates. *Polymers, 15*(1), 20. https://doi.org/10.3390/polym15010020

Hamed, M., Coelho, E., Bastos, R., Evtuguin, D. V., Ferreira, S. S., Lima, T., Vilanova, M., Sila, A., Coimbra, M. A., & Bougatef, A. (2022). Isolation and identification of an arabinogalactan extracted from pistachio external hull: Assessment of immunostimulatory activity. *Food Chemistry, 373*, Article 131416. https://doi.org/10.1016/j.foodchem.2021.131416

Ilyasov, I. R., Beloborodov, V. L., Selivanova, I. A., & Terekhov, R. P. (2020). ABTS/PP decolorization assay of antioxidant capacity reaction pathways. *International Journal of Molecular Sciences, 21*(3), 1131. https://doi.org/10.3390/ijms21031131

Imperio, D., Bordiga, M., Passos, C. P., Silva, S. P., Coimbra, M. A., Travaglia, F., Arlorio, M., Coïsson, J. D., & Panza, L. (2021). Gentianose: Purification and structural determination of an unknown oligosaccharide in grape seeds. *Food Chemistry, 344*, Article 128588. https://doi.org/10.1016/j.foodchem.2020.128588

Kong, L., Liu, Y., Zhi, P., Wang, X., Xu, B., Gong, Z., & Chang, C. (2020). Origins and evolution of cuticle biosynthetic machinery in land plants. *Plant Physiology, 184*(4), 1998–2010. https://doi.org/10.1104/pp.20.00913

Lee, H.-B., Kim, Y.-S., & Park, H.-Y. (2022). Pectic polysaccharides: Targeting gut microbiota in obesity and intestinal health. *Carbohydrate Polymers, 287*, Article 119363. https://doi.org/10.1016/j.carbpol.2022.119363

Li, Z., Zeng, J., Tong, Z., Qi, Y., & Gu, L. (2015). Hydrogenolytic depolymerization of procyanidin polymers from hi-tannin sorghum bran. *Food Chemistry, 188*, 337–342. https://doi.org/10.1016/j.foodchem.2015.05.021

Loewe-Muñoz, V., Balzarini, M., Delard, C., & Álvarez, A. (2019). Variability of stone pine (*Pinus pinea* L.) fruit traits impacting pine nut yield. *Annals of Forest Science, 76*(2), 1–10. https://doi.org/10.1007/S13595-019-0816-0/FIGURES/4

Lopes, G. R., Ferreira, A. S., Pinto, M., Passos, C. P., Coelho, E., Rodrigues, C., Figueira, C., Rocha, S. M., Nunes, F. M., & Coimbra, M. A. (2016). Carbohydrate content, dietary fibre and melanoidins: Composition of espresso from single-dose coffee capsules. *Food Research International, 89*, 989–996. https://doi.org/10.1016/j.foodres.2016.01.018

Lopes, G. R., Passos, C. P., Rodrigues, C., Teixeira, J. A., & Coimbra, M. A. (2020). Impact of microwave-assisted extraction on roasted coffee carbohydrates, caffeine, chlorogenic acids and coloured compounds. *Food Research International, 129*, Article 108864. https://doi.org/10.1016/j.foodres.2019.108864

López-Gambero, A. J., Sanjuan, C., Serrano-Castro, P. J., Suárez, J., & Rodríguez de Fonseca, F. (2020). The biomedical uses of inositols: A nutraceutical approach to metabolic dysfunction in aging and neurodegenerative diseases. *Biomedicines, 8*(9), 295. https://doi.org/10.3390/biomedicines8090295

Mandalari, G., Tomaino, A., Arcoraci, T., Martorana, M., Turco, V. Lo, Cacciola, F., Rich, G. T., Bisignano, C., Saija, A., Dugo, P., Cross, K. L., Parker, M. L., Waldron, K. W., & Wickham, M. S. J (2010). Characterization of polyphenols, lipids and dietary fibre from almond skins (*Amygdalus communis* L.). *Journal of Food Composition and Analysis, 23*(2), 166–174. https://doi.org/10.1016/j.jfca.2009.08.015

Mateos-Aparicio, I., De la Peña Armada, R., Pérez-Cózar, M. L., Rupérez, P., Redondo-Cuenca, A., & Villanueva-Suárez, M. J. (2020). Apple by-product dietary fibre exhibits potential prebiotic and hypolipidemic effects in high-fat fed Wistar rats. *Bioactive Carbohydrates and Dietary Fibre, 23*, Article 100219. https://doi.org/10.1016/j.bcdf.2020.100219

Minzanova, S., Mironov, V., Arkhipova, D., Khabibullina, A., Mironova, L., Zakirova, Y., & Milyukov, V. (2018). Biological activity and pharmacological application of pectic polysaccharides: A review. *Polymers, 10*(12), 1407. https://doi.org/10.3390/polym10121407

Mohnen, D. (2008). Pectin structure and biosynthesis. *Current Opinion in Plant Biology, 11*(3), 266–277. https://doi.org/10.1016/j.pbi.2008.03.006

Moshtaghian, H., Bolton, K., & Rousta, K. (2021). Challenges for upcycled foods: Definition, inclusion in the food waste management hierarchy and public acceptability. *Foods (Basel, Switzerland), 10*(11), 2874. https://doi.org/10.3390/foods10112874

Nunes, F. M., & Coimbra, M. A. (2002). Chemical characterization of the high-molecular-weight material extracted with hot water from green and roasted robusta coffees as affected by the degree of roast. *Journal of Agricultural and Food Chemistry, 50*(24), 7046–7052. https://doi.org/10.1021/jf020534e

Nunes, F. M., Reis, A., Silva, A. M. S., Domingues, M. R. M., & Coimbra, M. A. (2008). Rhamnoarabinosyl and rhamnoarabinoarabinosyl side chains as structural features of coffee arabinogalactans. *Phytochemistry, 69*(7), 1573–1585. https://doi.org/10.1016/j.phytochem.2008.01.021

Özdemir, K. S., Yılmaz, C., Durmaz, G., & Gökmen, V. (2014). Hazelnut skin powder: A new brown colored functional ingredient. *Food Research International, 65*, 291–297. https://doi.org/10.1016/j.foodres.2014.01.060

Pant, A. F., Özkasikci, D., Fürtauer, S., & Reinelt, M. (2019). The effect of deprotonation on the reaction kinetics of an oxygen scavenger based on gallic acid. *Frontiers in Chemistry, 7*, Article 470241. https://doi.org/10.3389/fchem.2019.00680

Passos, C. P., & Coimbra, M. A. (2013). Microwave superheated water extraction of polysaccharides from spent coffee grounds. *Carbohydrate Polymers, 94*(1), 626–633. https://doi.org/10.1016/j.carbpol.2013.01.088

Pękala, P., Szymańska-Chargot, M., & Zdunek, A. (2023). Interactions between non-cellulosic plant cell wall polysaccharides and cellulose emerging from adsorption studies. *Cellulose (London, England), 30*, 9221–9239. https://doi.org/10.1007/s10570-023-05442-y

Piqué, N., Gómez-Guillén, M., & Montero, M. (2018). Xyloglucan, a plant polymer with barrier protective properties over the mucous membranes: An overview. *International Journal of Molecular Sciences, 19*(3), 673. https://doi.org/10.3390/ijms19030673

Queirós, C. S. G. P., Cardoso, S., Lourenço, A., Ferreira, J., Miranda, I., Lourenço, M. J. V., & Pereira, H. (2020). Characterization of walnut, almond, and pine nut shells regarding chemical composition and extract composition. *Biomass Conversion and Biorefinery, 10*, 175–188. https://doi.org/10.1007/s13399-019-00424-2

Ravber, M., Knez, Ž., & Škerget, M. (2015). Simultaneous extraction of oil- and water-soluble phase from sunflower seeds with subcritical water. *Food Chemistry, 166*, 316–323. https://doi.org/10.1016/j.foodchem.2014.06.025

Razeq, F. M., Kosma, D. K., França, D., Rowland, O., & Molina, I. (2021). Extracellular lipids of *Camelina sativa*: Characterization of cutin and suberin reveals typical polyester monomers and unusual dicarboxylic fatty acids. *Phytochemistry, 184*, Article 112665. https://doi.org/10.1016/j.phytochem.2021.112665

Re, R., Pellegrini, N., Proteggente, A., Pannala, A., Yang, M., & Rice-Evans, C. (1999). Antioxidant activity applying an improved ABTS radical cation decolorization assay. *Free Radical Biology and Medicine, 26*(9–10), 1231–1237. https://doi.org/10.1016/S0891-5849(98)00315-3

Reis, S. F., Lopes, P., Roseira, I., Cabral, M., Mateus, N., & Freitas, V. (2019). Recovery of added value compounds from cork industry by-products. *Industrial Crops and Products, 140*, Article 111599. https://doi.org/10.1016/j.indcrop.2019.111599

Reis, S. F., Martins, V. J., Bastos, R., Lima, T., Correia, V. G., Pinheiro, B. A., … Coelho, E. (2023). Feasibility of brewer's spent yeast microcapsules as targeted oral carriers. *Foods, 12*(2), 246. https://doi.org/10.3390/FOODS12020246/S1

Reynoud, N., Petit, J., Bres, C., Lahaye, M., Rothan, C., Marion, D., & Bakan, B. (2021). The complex architecture of plant cuticles and its relation to multiple biological functions. *Frontiers in Plant Science, 12*, Article 782773. https://doi.org/10.3389/fpls.2021.782773

Roupar, D., Coelho, M. C., Gonçalves, D. A., Silva, S. P., Coelho, E., Silva, S., … Nobre, C. (2022). Evaluation of microbial-fructo-oligosaccharides metabolism by human gut

microbiota fermentation as compared to commercial inulin-derived oligosaccharides. *Foods, 11*(7), 954. https://doi.org/10.3390/foods11070954

Seraglio, S. K. T., Valese, A. C., Daguer, H., Bergamo, G., Azevedo, M. S., Nehring, P., Gonzaga, L. V., Fett, R., & Costa, A. C. O. (2017). Effect of *in vitro* gastrointestinal digestion on the bioaccessibility of phenolic compounds, minerals, and antioxidant capacity of *Mimosa scabrella* Bentham honeydew honeys. *Food Research International, 99*, 670–678. https://doi.org/10.1016/j.foodres.2017.06.024

Silva, S. P., Coreta-Gomes, F., Coimbra, M. A., & Coelho, E. (2024). Pine nut skin as a source of phytosterols and alkanediols - Hypocholesterolemic potential and development of sustainable vegan emulsifiers. *LWT, 197*, Article 115934. https://doi.org/10.1016/j.lwt.2024.115934

Silva, S. P., Moreira, A. S. P., Domingues, M., do, R. M., Evtuguin, D. V., Coelho, E., & Coimbra, M. A. (2019). Contribution of non-enzymatic transglycosylation reactions to the honey oligosaccharides origin and diversity. *Pure and Applied Chemistry, 91*(7), 1231–1242. https://doi.org/10.1515/pac-2019-0209

Simões, J., Maricato, É., Nunes, F. M., Domingues, M. R., & Coimbra, M. A. (2014). Thermal stability of spent coffee ground polysaccharides: Galactomannans and arabinogalactans. *Carbohydrate Polymers, 101*, 256–264. https://doi.org/10.1016/j.carbpol.2013.09.042

Singleton, V. L., & Rossi, J. A. (1965). Colorimetry of total phenolics with phosphomolybdic-phosphotungstic acid reagents. *American Journal of Enology and Viticulture, 16*(3), 144–158. https://doi.org/10.5344/ajev.1965.16.3.144

Smith, R. M. (2002). Extractions with superheated water. *Journal of Chromatography A, 975*, 31–46. https://doi.org/10.1016/S0021-9673(02)01225-6

Stribling, P., & Ibrahim, F. (2023). Dietary fibre definition revisited - The case of low molecular weight carbohydrates. *Clinical Nutrition ESPEN, 55*, 340–356. https://doi.org/10.1016/j.clnesp.2023.04.014

Sun, B., Ricardo-da-Silva, J. M., & Spranger, I. (1998). Critical factors of vanillin assay for catechins and proanthocyanidins. *Journal of Agricultural and Food Chemistry, 46*(10), 4267–4274. https://doi.org/10.1021/jf980366j

Tuomivaara, S. T., Yaoi, K., O'Neill, M. A., & York, W. S. (2015). Generation and structural validation of a library of diverse xyloglucan-derived oligosaccharides, including an update on xyloglucan nomenclature. *Carbohydrate Research, 402*, 56–66. https://doi.org/10.1016/j.carres.2014.06.031

Zhao, M. Y., Ju, T., Ling, X. X., Dai, Y., & Zhao, Y. H. (2017). Component analysis of pine nut skin and its application in yogurt. *Modern Food Science and Technology, 33*(7), 133–140. https://doi.org/10.13982/j.mfst.1673-9078.2017.7.020